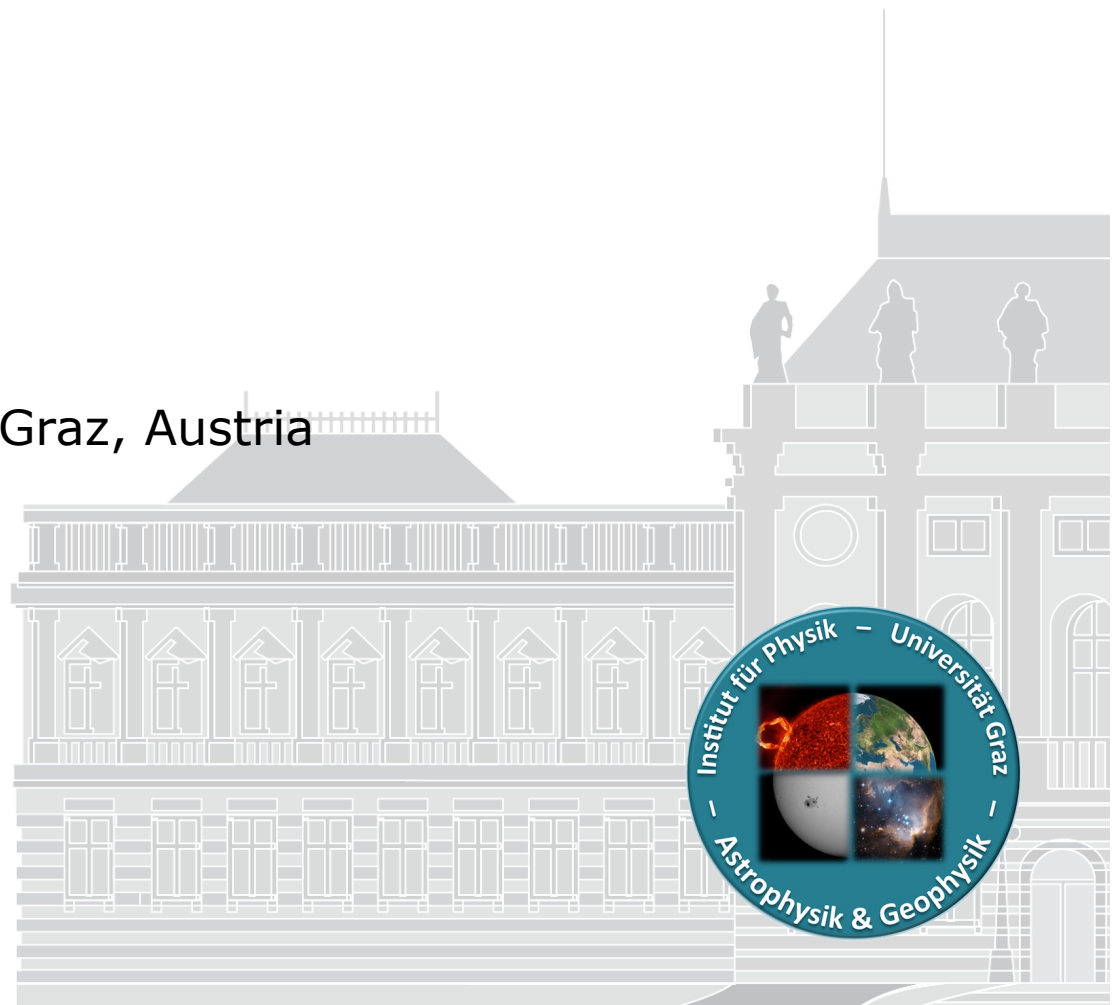
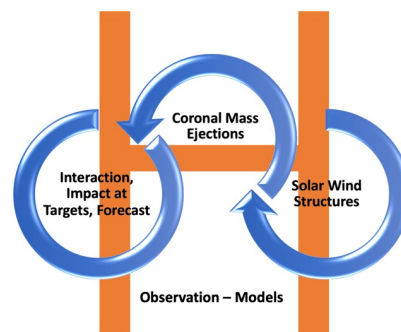


CMEs and their Impact on Space Weather

Manuela Temmer

Institute of Physics, University of Graz, Austria

swe.uni-graz.at



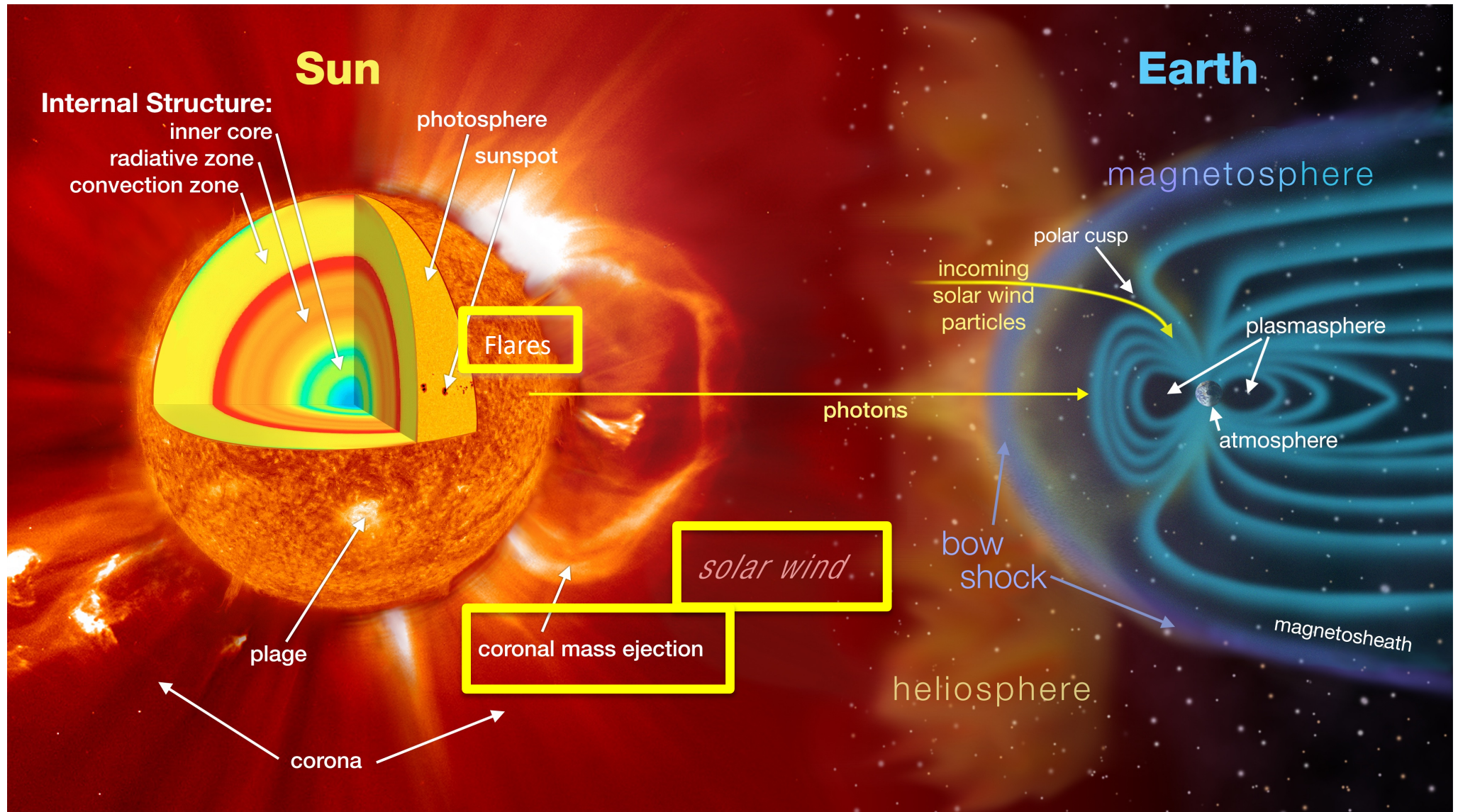
ISSS @ L'Aquila :: April 15, 2022 ::

CMEs, flares, SEPs
—
the solar perspective

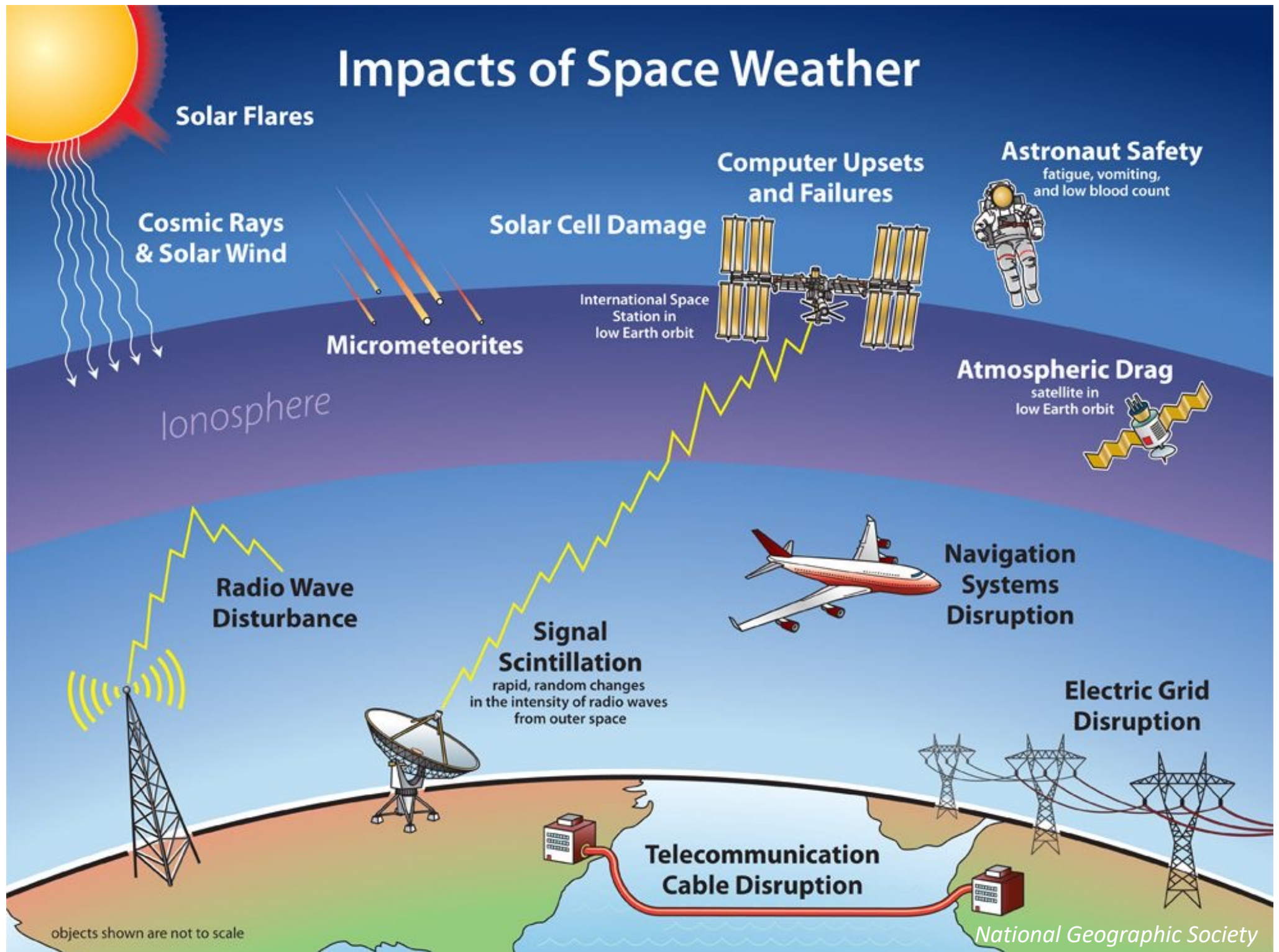
Space-Weather = Solar-terrestrial physics



Solar physics -> Heliospheric physics -> Geospace (Magnetosphere, Ionosphere, Thermosphere, Surface)

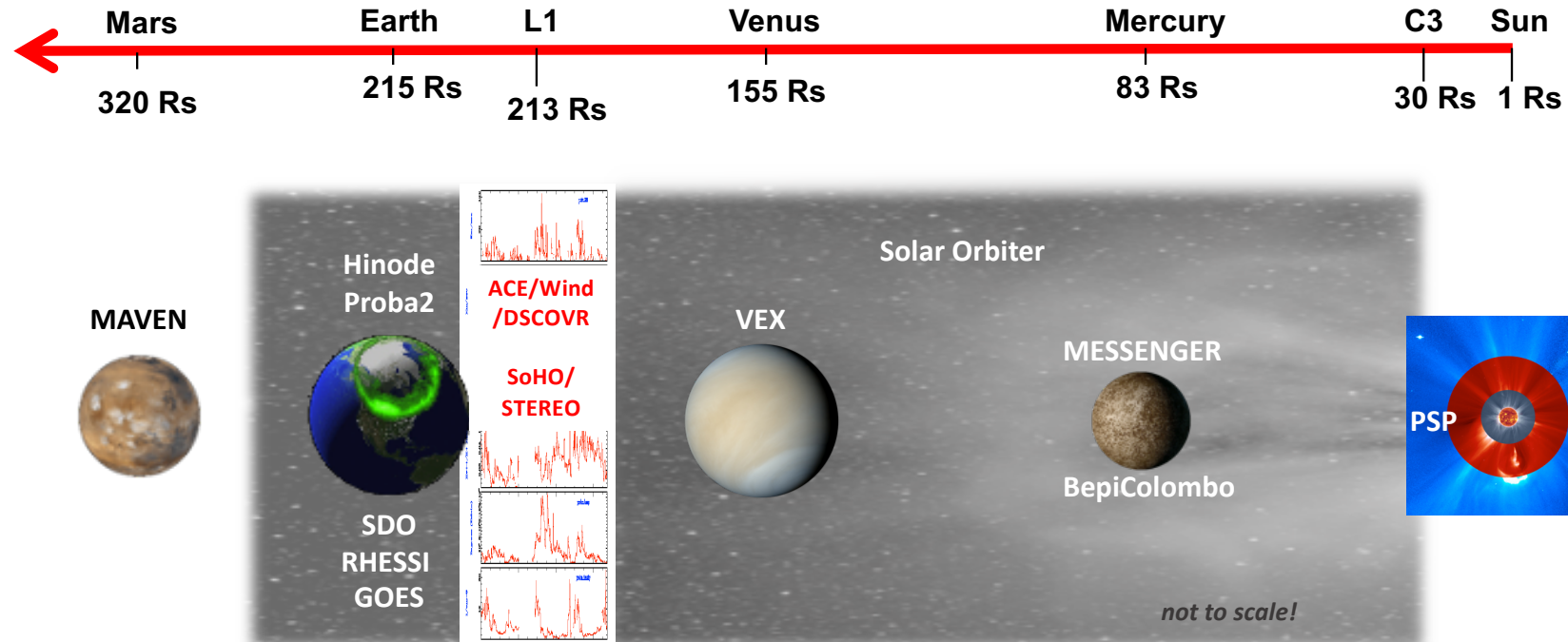


Impacts of Space Weather



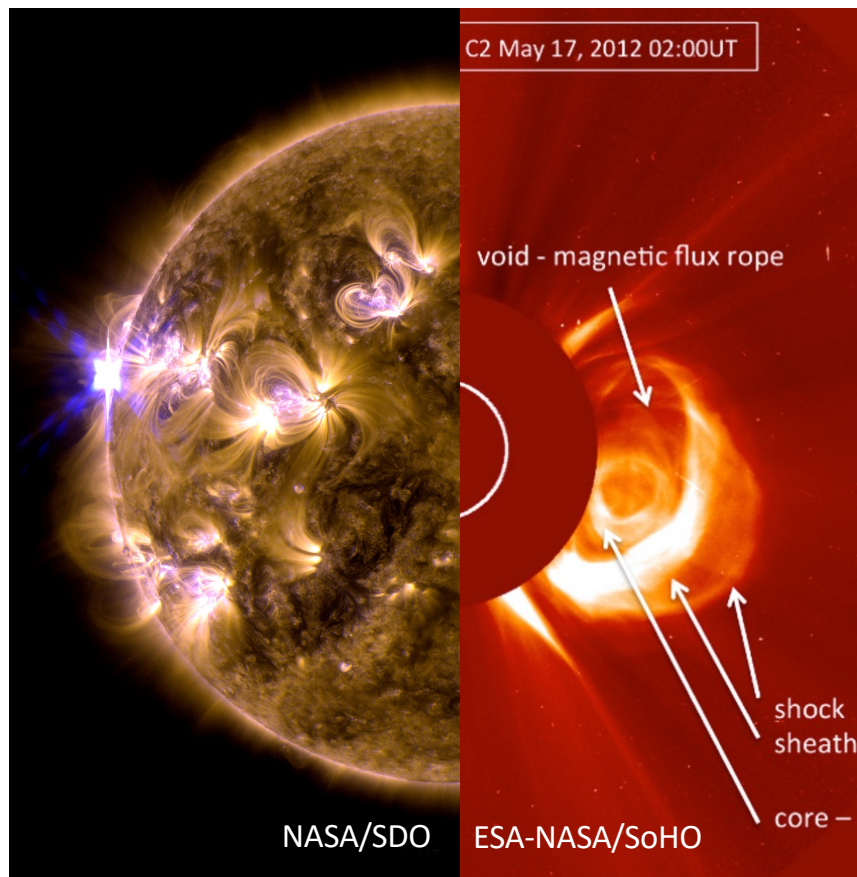
Data: remote-sensing and in-situ

- Remote data for observations of the solar surface and magnetic field
- Coronagraphs (SoHO since 1996, STEREO since 2006): FoV up to 30Rs, STEREO HI1+2 inner heliosphere
- ACE/Wind in-situ (since 1994), DSCOVR (since 2015) at L1
- In-situ instruments at planet's orbit (Venus Express (2005-2014), MESSENGER (2004-2015), MAVEN, BepiColombo)
- Variable distances and off-ecliptic: **Parker Solar Probe** (since 2018) and **Solar Orbiter** (since 2020)



Temmer, 2021 (Living Reviews)

Solar activity: Flares and CMEs



CMEs arise from usually complex, closed magnetic field structures. Some instability disrupts the equilibrium causing an eruption (e.g., [Forbes 2000](#)).

CMEs related to flares – magnetic reconnection strongly drives the CME.

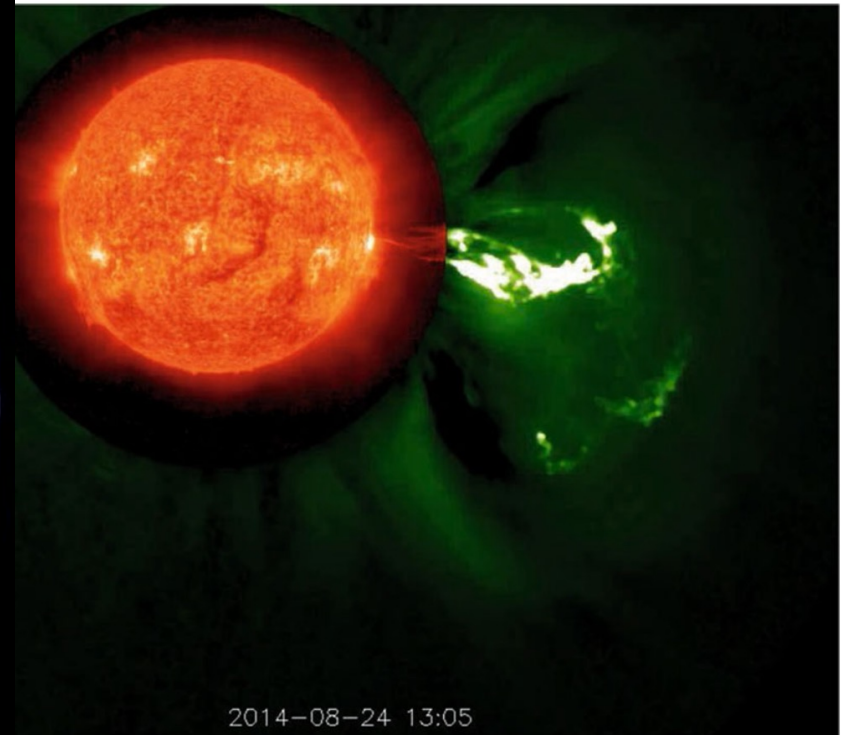
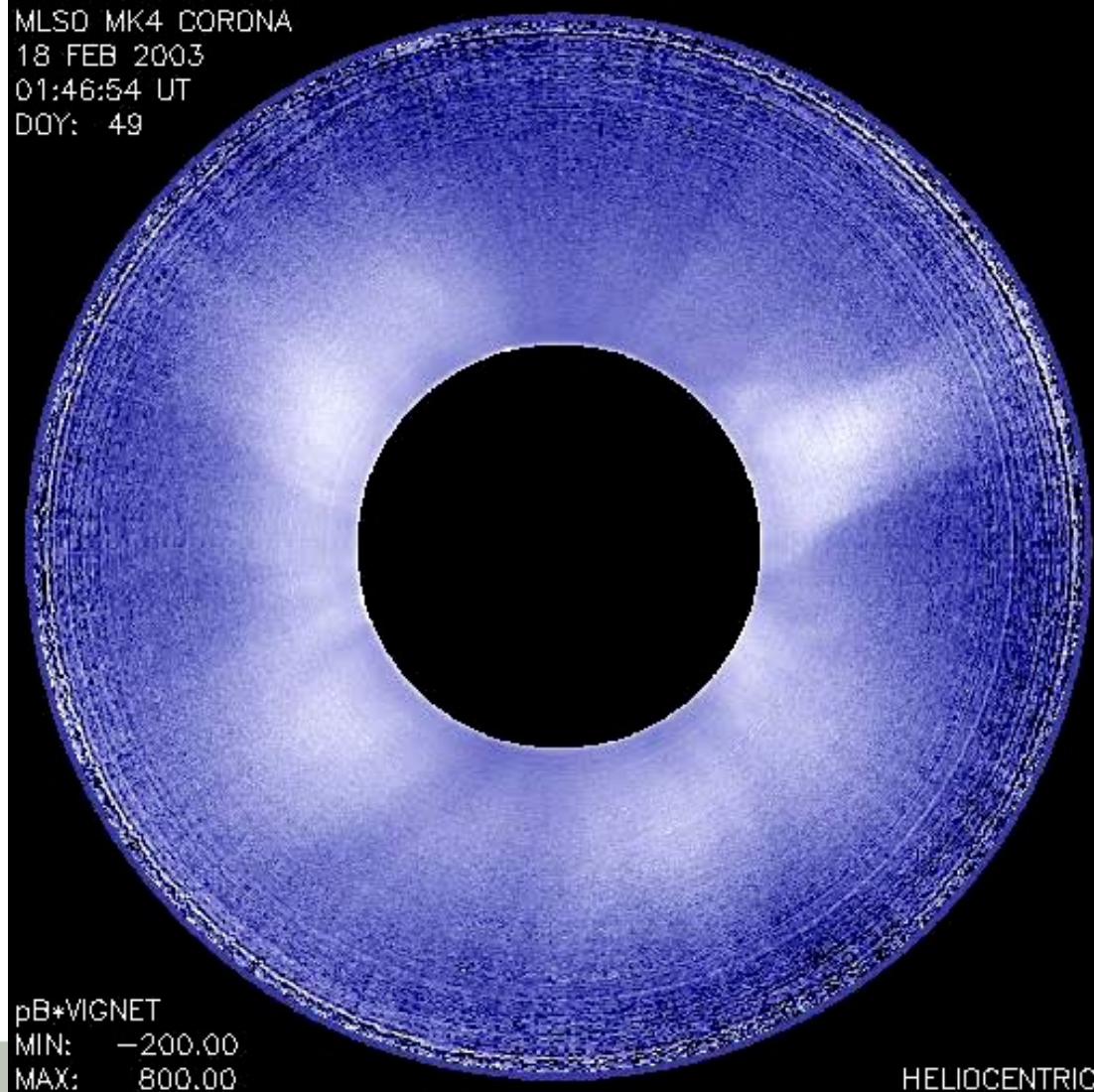
CMEs erupting in high corona due to simple field reconfiguration ('stealth' CMEs, [Robbrecht+ 2009](#); [D'Huys+ 2014](#); [Nitta & Mulligan, 2020](#)).

Confined events may show strong emission but no mass ejection (e.g., [Sun+2015](#), [Thalmann+ 2015](#)).

Mid-corona – where major changes happen



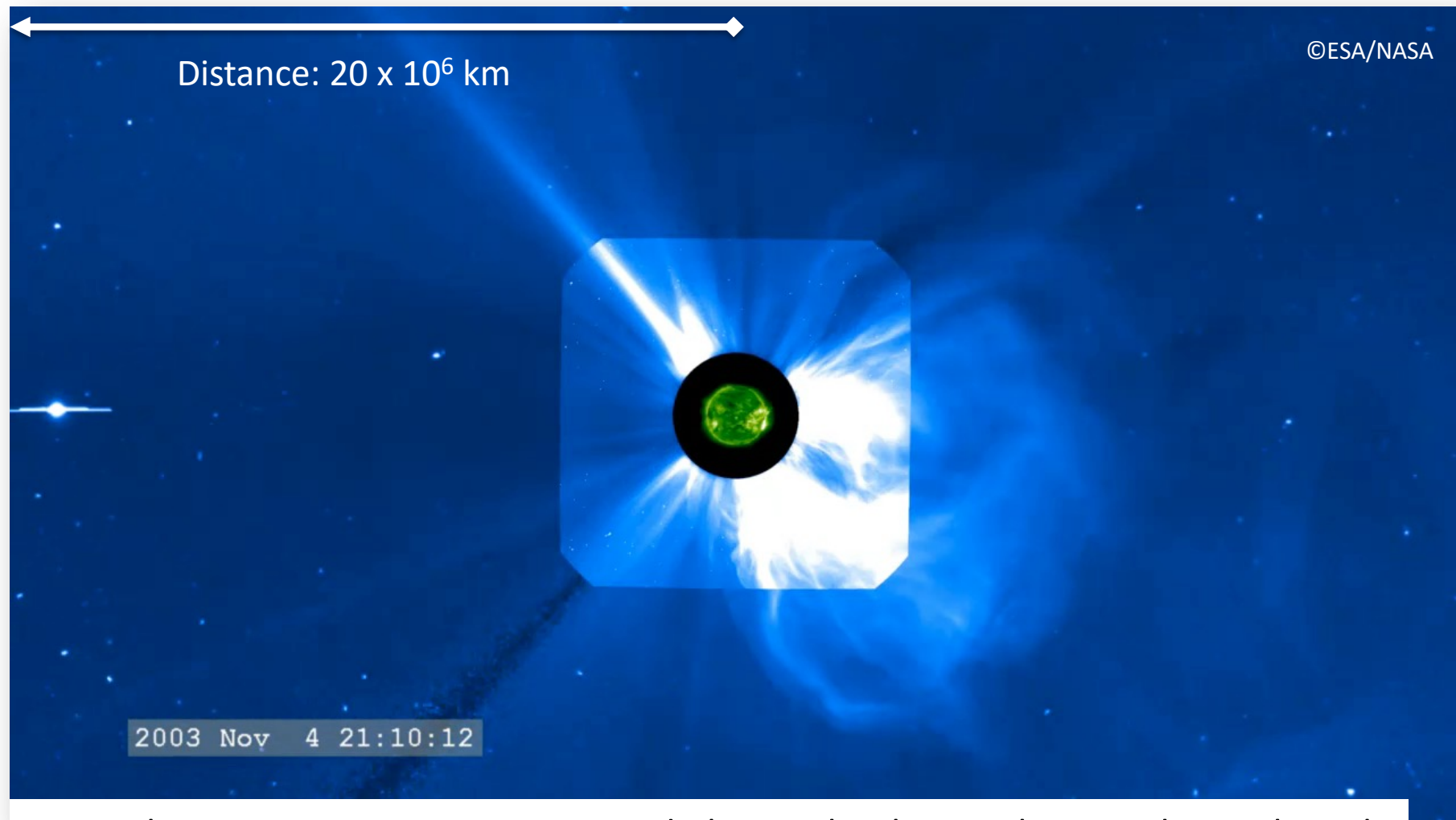
<http://middlecorona.com/instruments.html>



Combining instruments: EUV
and white-light

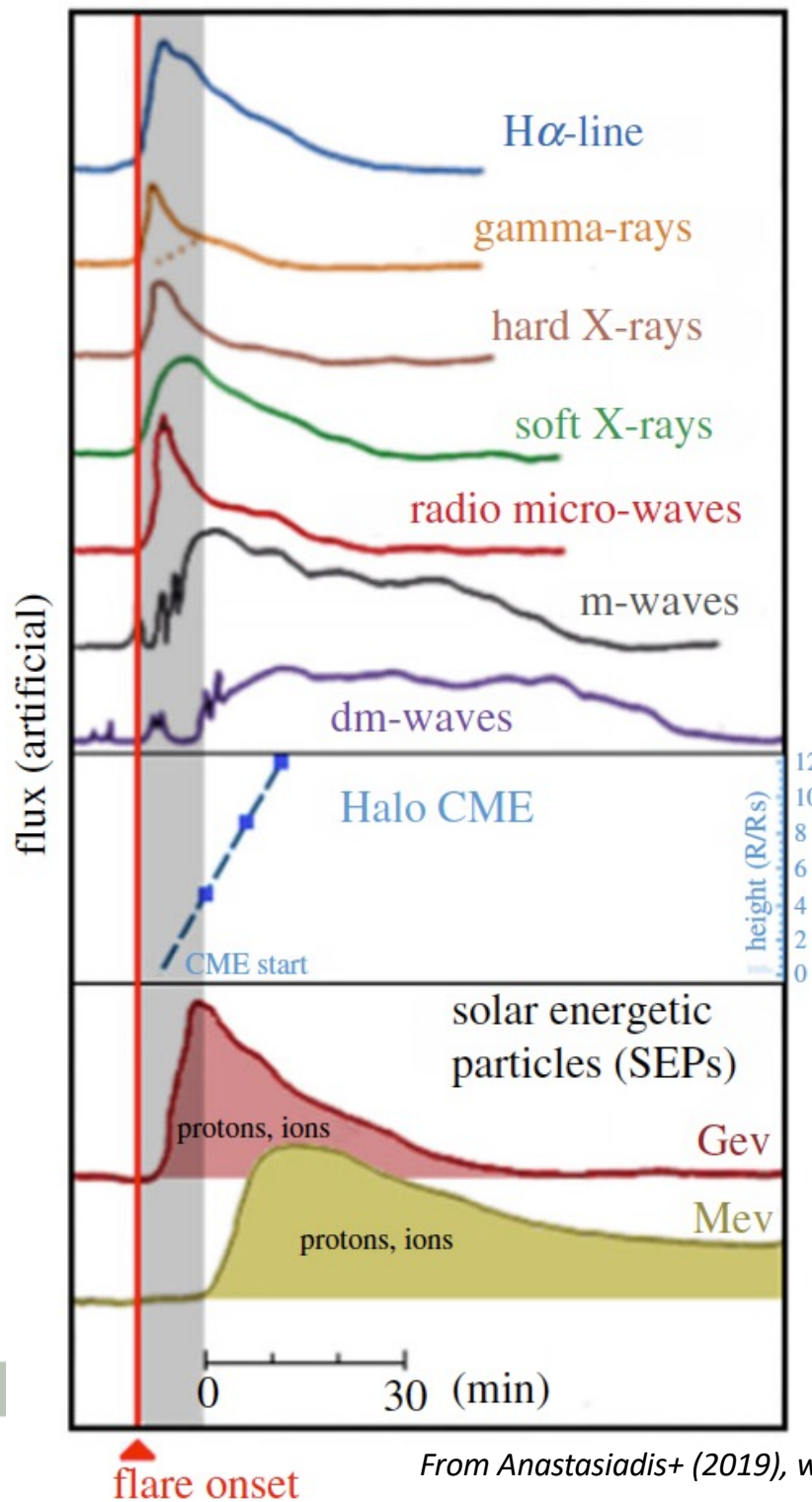
UNIVERSITY OF GRAZ

Eruptive events: coronal mass ejections



Coronal mass ejections are magnetized plasma that leaves the Sun abruptly with speeds from about 400 km/s up to 3000 km/s. Those disturbances propagate the Sun-Earth distance in ca. 1-4 days and may be geoeffective.

Flare-CME-SEP relation

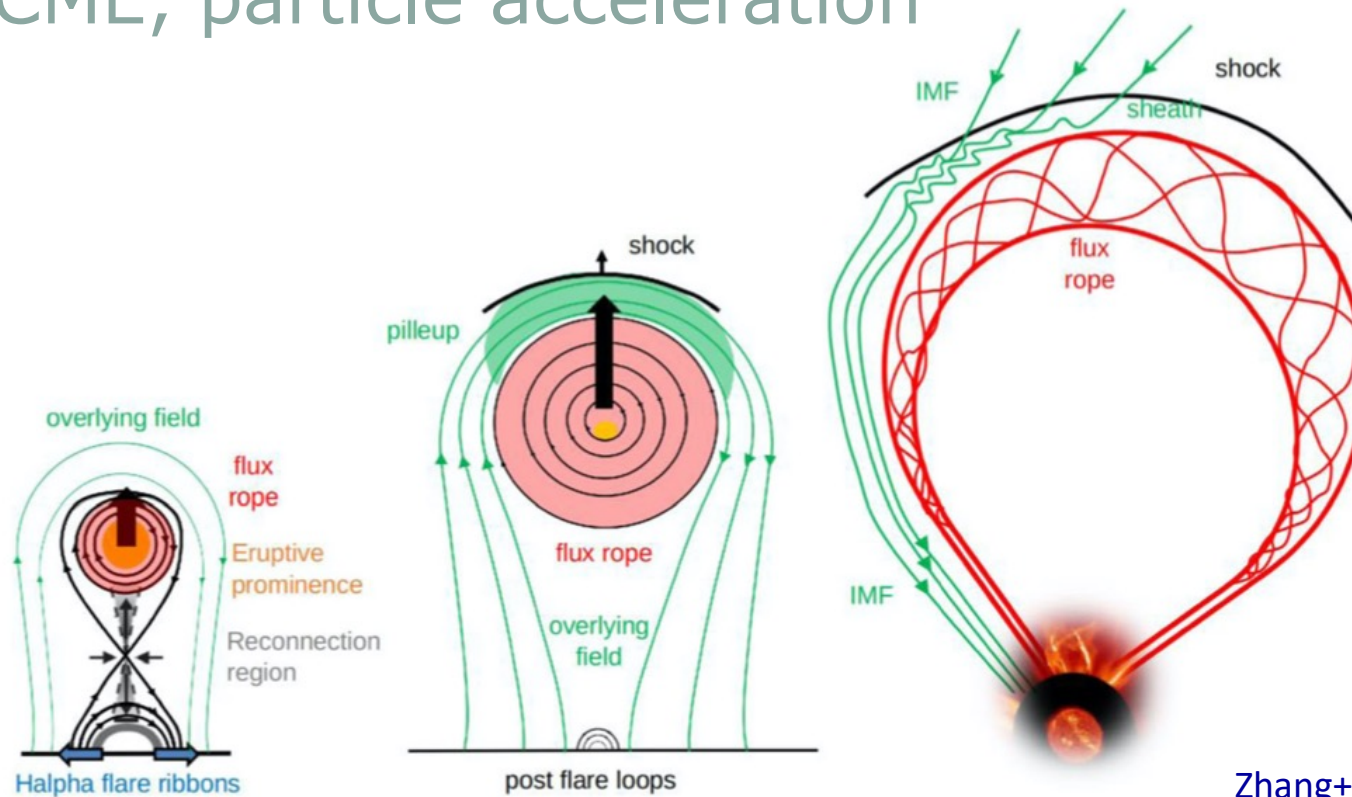


Pre-flare phase - thermal emission in SXR and EUV, H-alpha kernel brightenings. If related to a filament eruption, this phase partly coincides with the slow rise phase of the filament.

Impulsive flare phase - non-thermal emission in hard X-ray (HXR) due to particles accelerating out of the localized reconnection area (Review see e.g., Fletcher et al. 2011). Now also the CME body forms when magnetic field lines close in the upper part of the reconnection area r (flux rope structure). SEP flux in the GeV energy range starts to rise.

Decay phase – back to pre-flare level

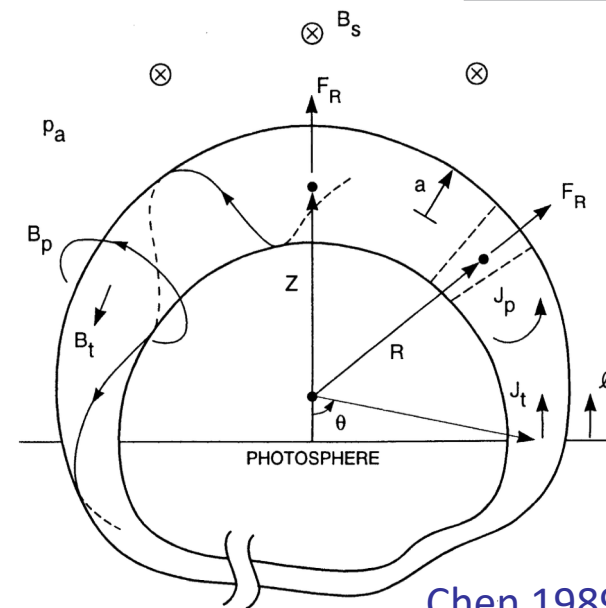
Flare, CME, particle acceleration



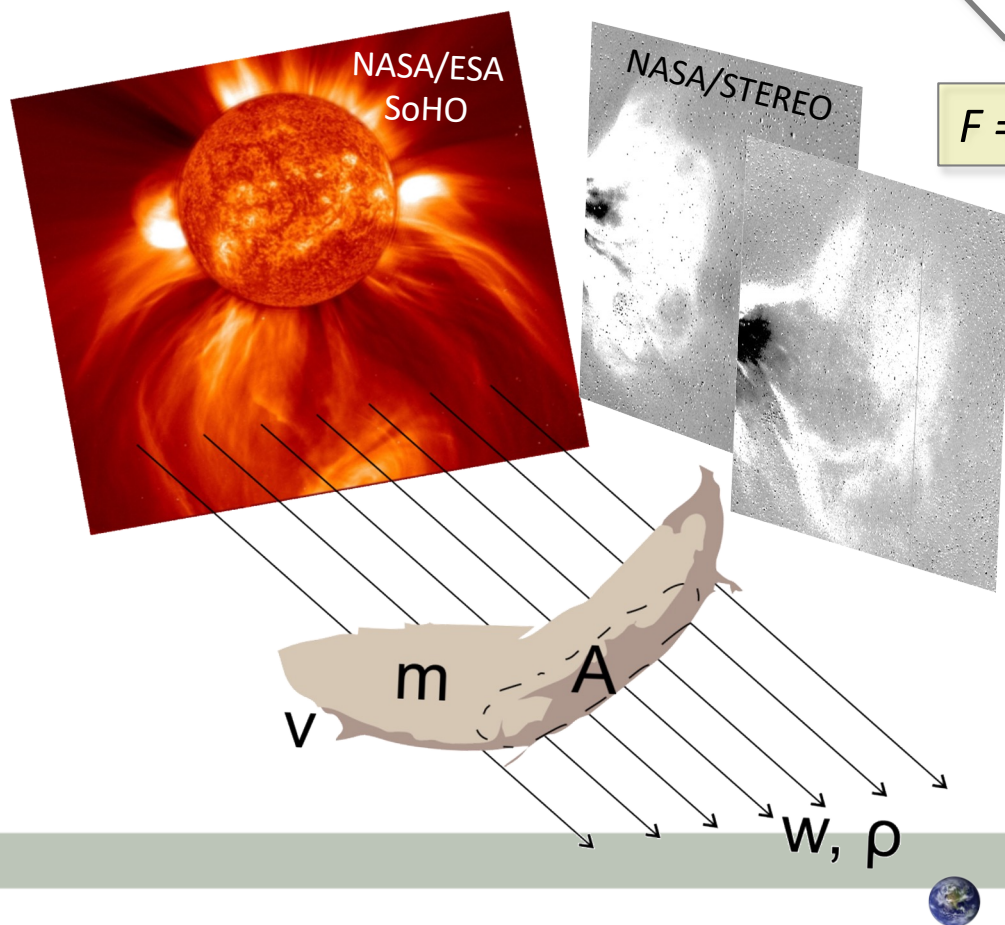
- Major Space Weather contributors:
 - Flares – radiation, radio blackouts
 - CMEs – geomagnetic storms, reconnection and compression of magnetosphere
 - SIR/CIR – geomagnetic storms, dB/dt variation
 - SEPs – trigger of SPE, radiation hazard
- Flare/CME trigger mechanisms see e.g., reviews by [Schmieder+ 2015](#); [Green+ 2018](#)

CME driving forces

Close to the Sun propelling *Lorentz (hoop) force* as consequence of mag. reconn. $>B_p > I_t \Rightarrow F_R > 0$ (see e.g. J. Chen 1989,1996; Kliem & Török 2006)



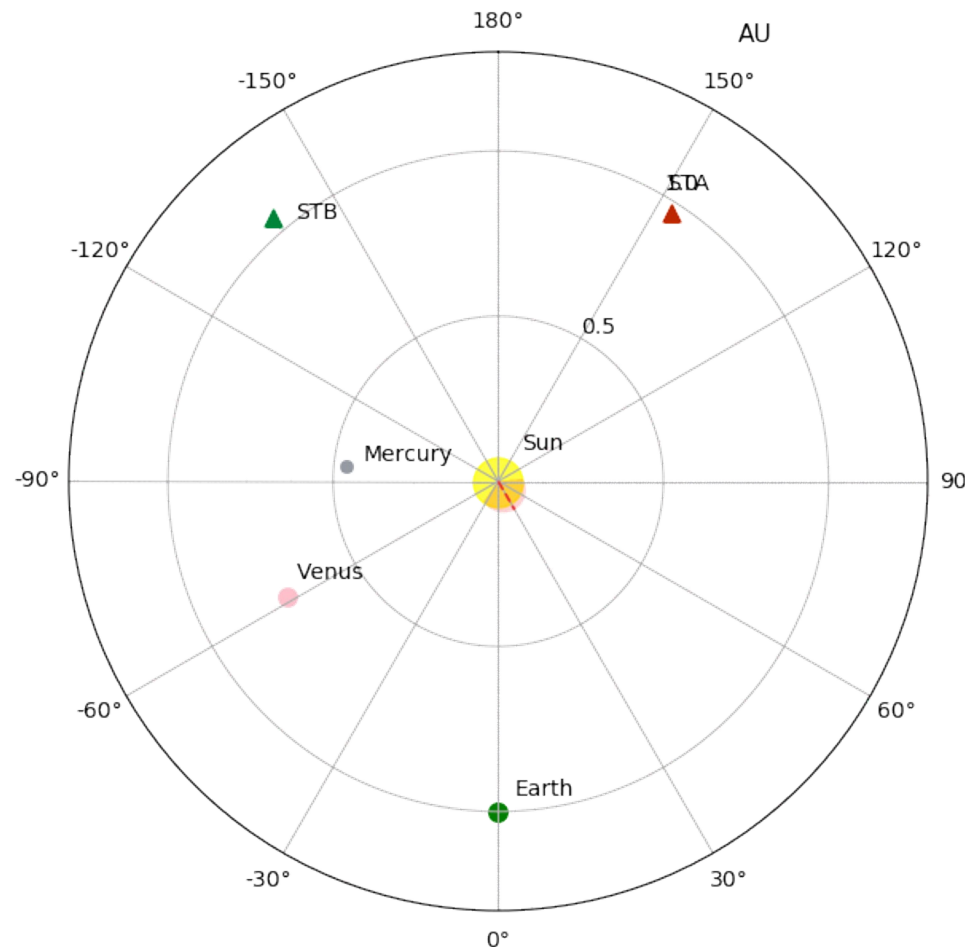
$$F = F_L + F_G + F_D$$



In IP space *drag* acceleration due to ambient SW flow (e.g. Cargill+ 1996; J. Chen, 1996; Vršnak+ 2004)

$$F_D = C_D A \frac{\rho V^2}{2}$$

Analytical drag-based models



Animation info

Date: 30 Sep 2013
Time: 01:45 h
Transit time: 0.0 h
Speed, v : 949 km/s
Distance: 0.09 AU

DBM results

CME arrival (at Earth)
Date: 02 Oct 2013
Time: 08:56 h
Transit time: 55.18 h
Speed at target: 575 km/s
Distance (target): 1.0 AU

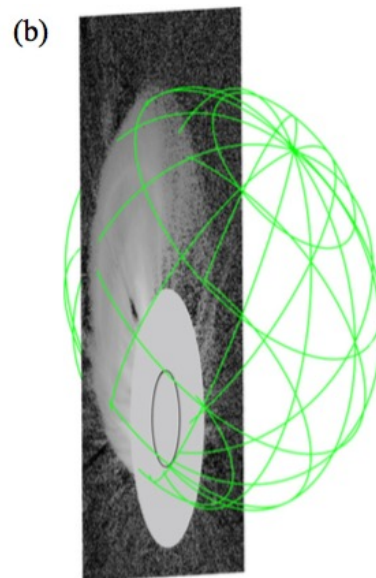
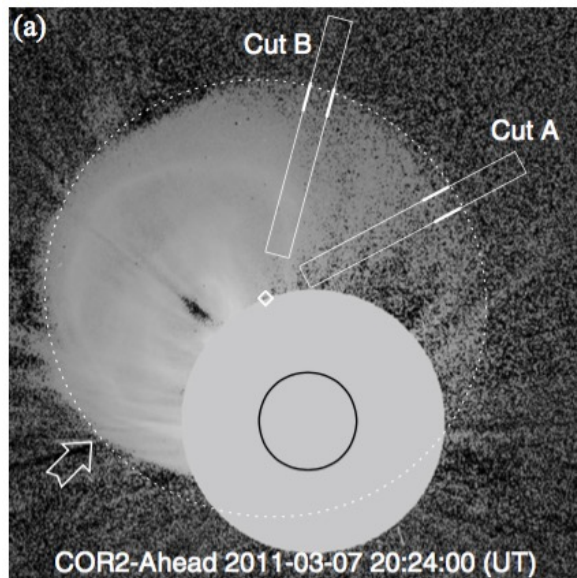
Input parameters

CME date: 30 Sep 2013
CME time: 01:45 h
Drag, γ : $0.3 \times 10^{-7} \text{ km}^{-1}$
SW speed, w : 450 km/s
Radial dist., R_0 : $21.5 r_{Sun}$
CME init. speed, v_0 : 1000 km/s
CME half-width, λ : 66.0 deg
CME long., ϕ_{CME} : 30.0 deg
Target: Earth

figure generated with DBEMv3

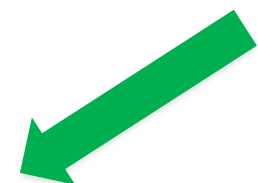
Drag coefficient (C_D), CME cross-section (A), density, and speed at an initial distance are used as input for running DB(E)M. See [Vrsnak, Zic, Vrbanec, Temmer+ 2013](#); [Zic, Vrsnak, Temmer, 2015](#); [Dumbovic+ 2018](#); [Calogovic+ 2021](#)

CMEs: what do we actually observe?



Kwon & Vourlidas 2018

Shock (sheath)



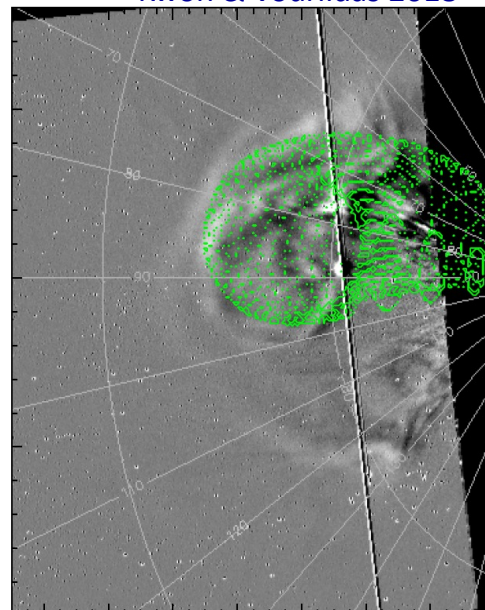
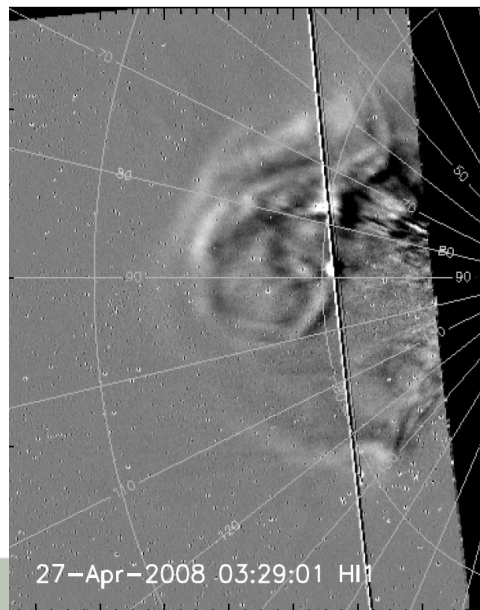
- CMEs are optically thin.
- Projection effects influence measurements severely.
- Compressed shock region, leading edge and magnetic driver (flux rope).
- Driver part: intense storms if strong negative B_z

(see e.g., [Burkepile+2004](#); [Cremades & Bothmer, 2004](#); [Kwon+2015](#); [Kilpua+2015](#)).

Magnetic flux rope (driver)



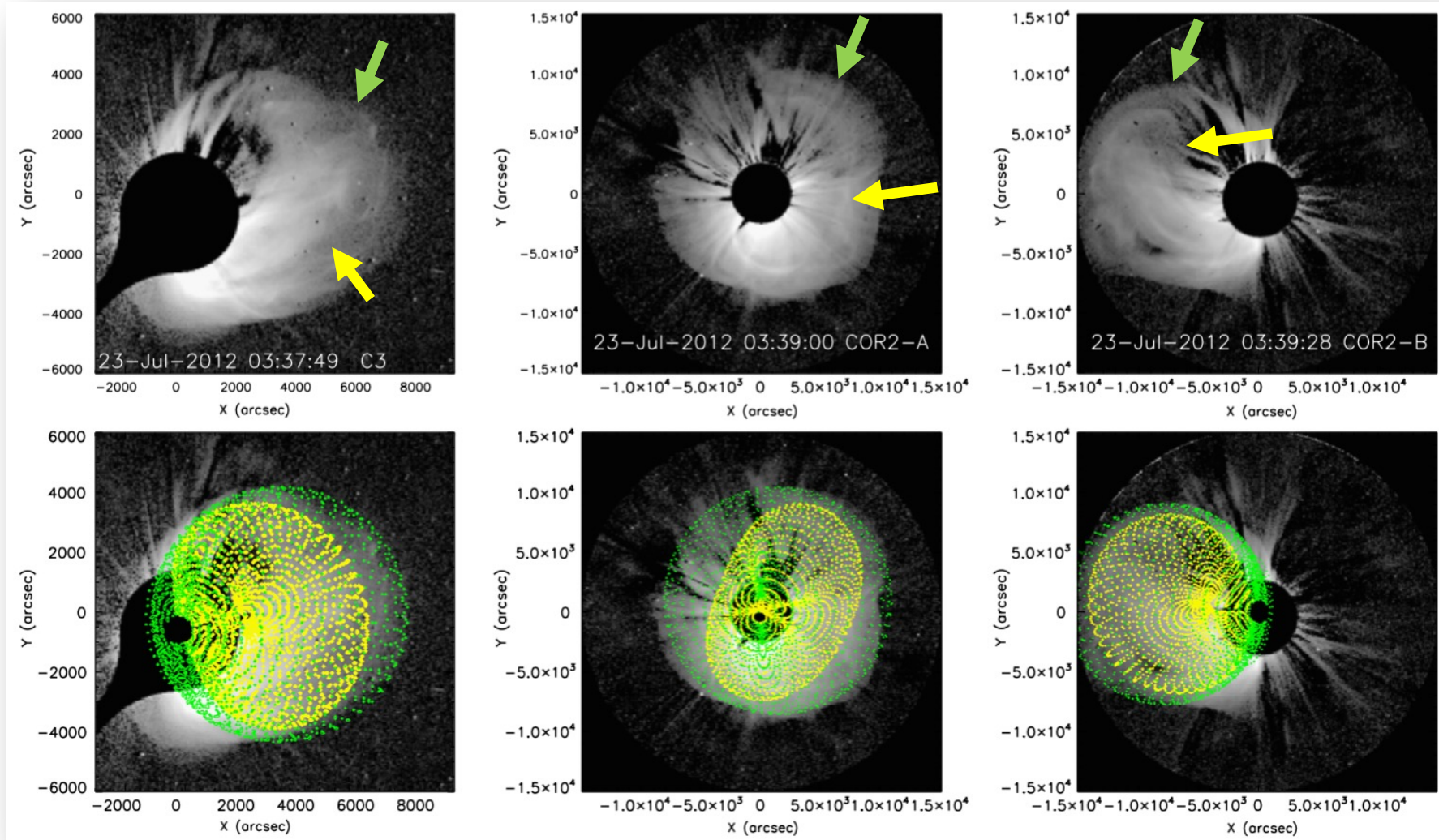
Temmer+ in prep.



Reconstructing CME geometry with multi-s/c data



Temmer & Nitta, 2015



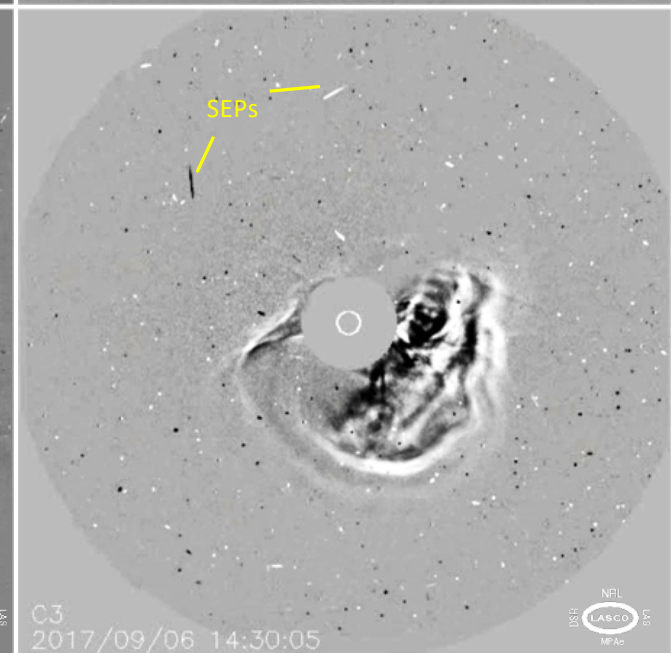
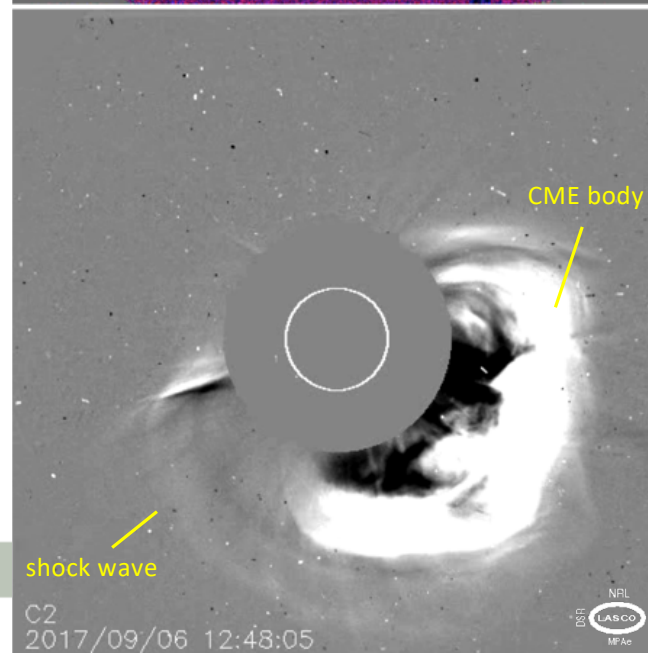
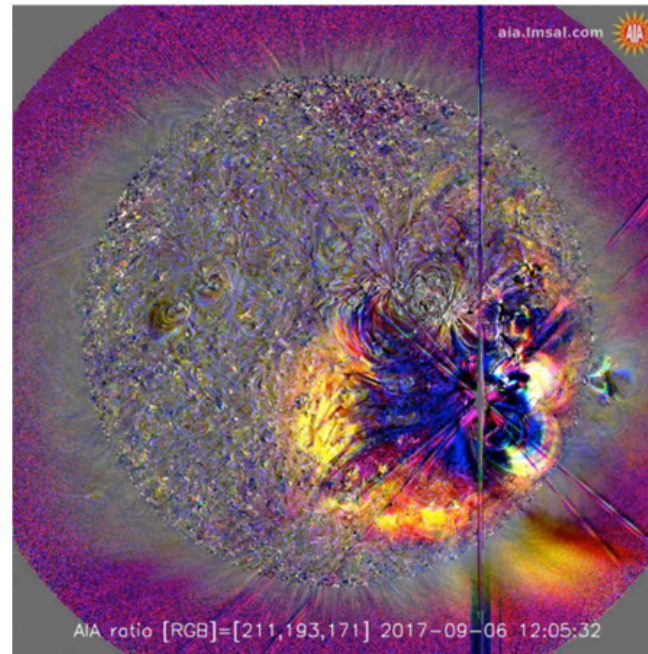
Flares, CMEs and SEPs – Sep 2017 events



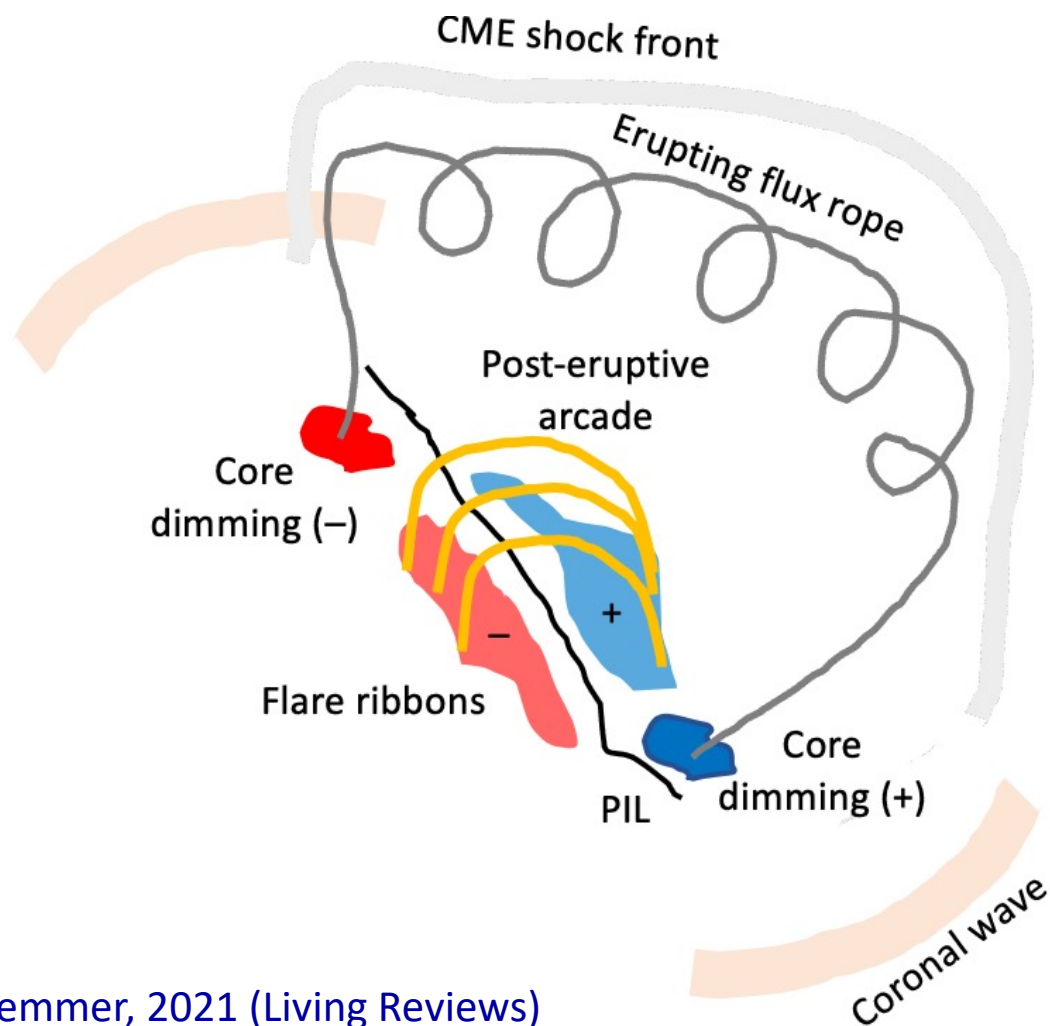
The generated SEPs are accelerated to relativistic speeds producing spikes in the image data (“snowstorm” effect).

This event was the first flare event in a sequence of X-class flares on 6, 7, and 10 September 2017 causing strong disturbances at Earth and Mars.

This is the most well documented Space Weather event from solar cycle 25.



Solar surface phenomena related to an eruptive event



- **Flare** – bright H-alpha, EUV, SXR, HXR, white-light for strong events
- **Mass release** – EUV dimming regions, radio type III bursts
- **Flux rope formation** and lift off – filament eruption and mass motion
- **Propagating surface wave** due to laterally expanding shock

Temmer, 2021 (Living Reviews)

Early CME evolution - connecting to the solar surface



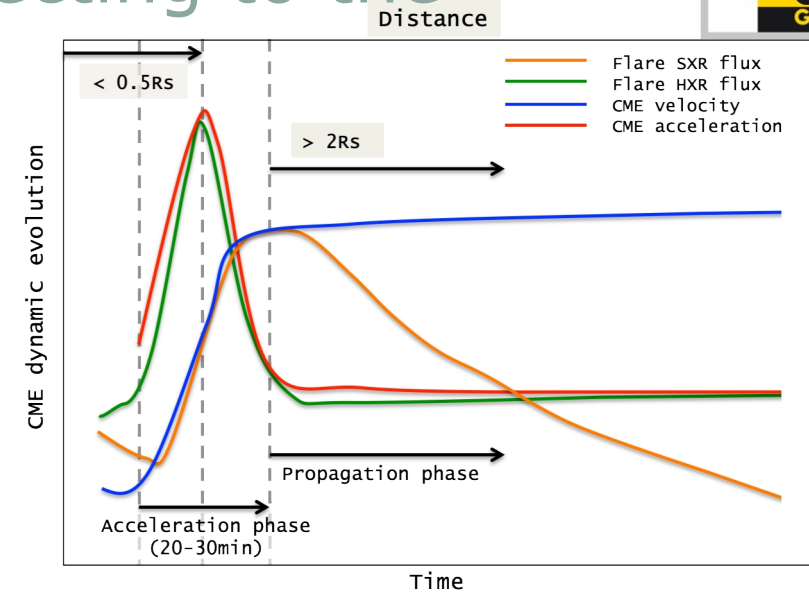
Temmer 2016

Flare-CME feedback relation:

HXR flare \Leftrightarrow *CME acceleration*

SXR flare \Leftrightarrow *CME speed*

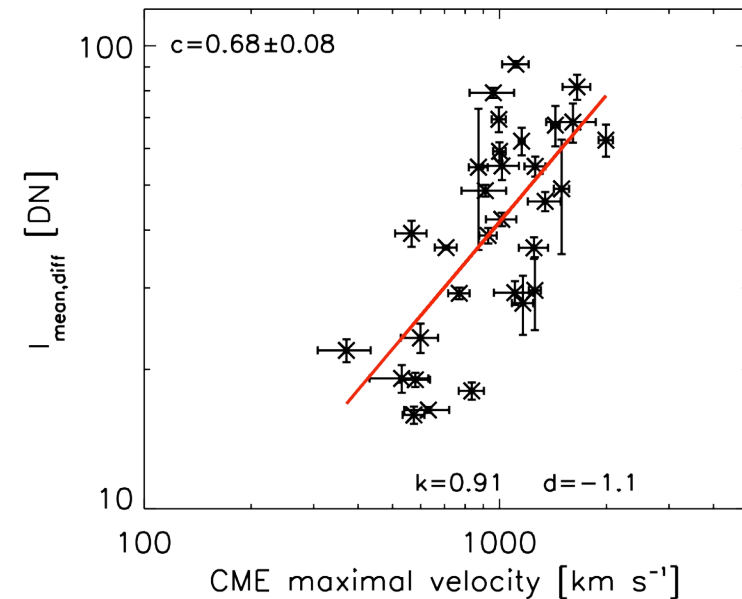
(e.g., Zhang+ 2001, 2004;
Chen & Krall, 2003; Maričić+ 2007;
Temmer+ 2008, 2010).



Mass depletion is observed as dimming in EUV (e.g., Hudson & Cliver, 2001; Mandrini+2007).

Core dimmings – CME footpoints (e.g., Temmer+2017).

Dimming intensity – CME speed relation (Dissauer+ 2018, 2019).



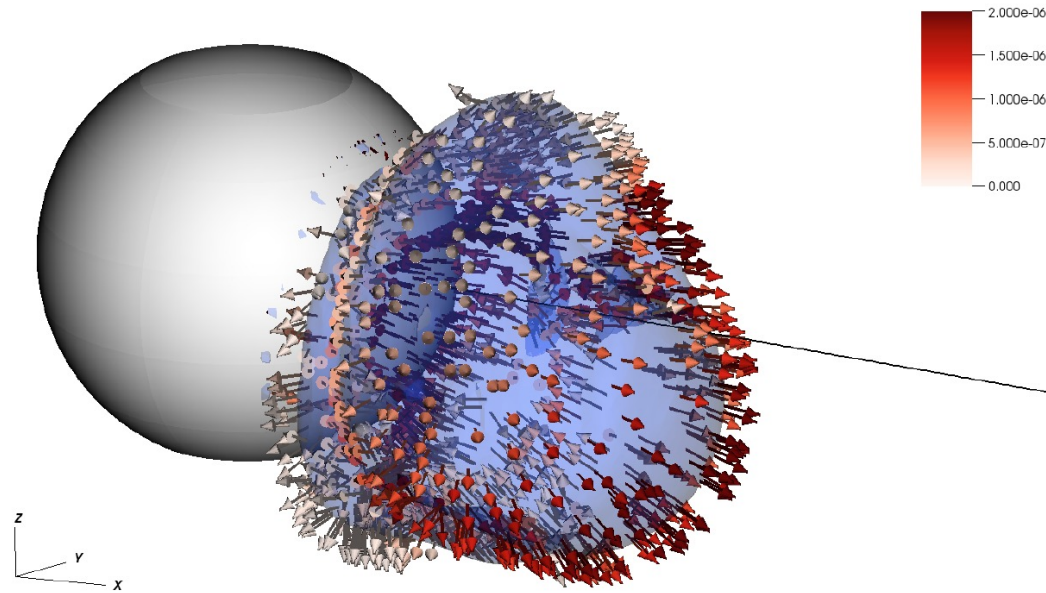
Dissauer+ 2019

CME-related surface parameters can make a major contribution to detect CMEs and derive their characteristics before entering a coronagraph FoV.

EUHFORIA – spheromak model

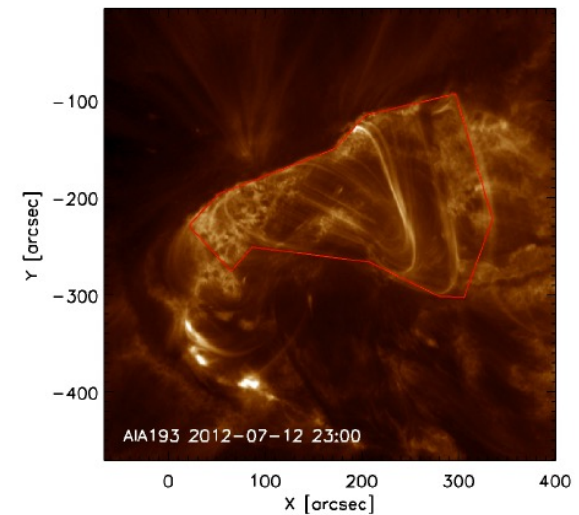
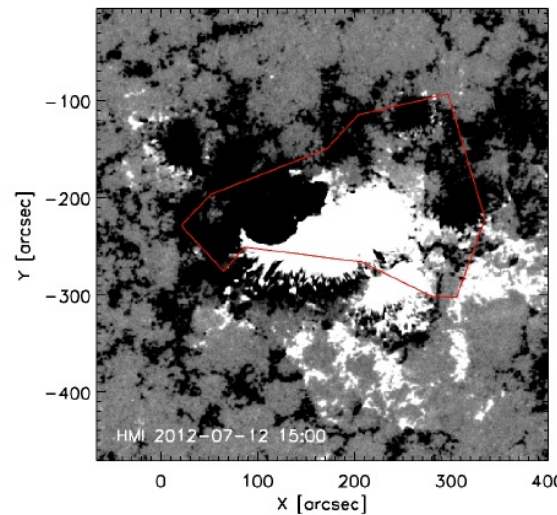
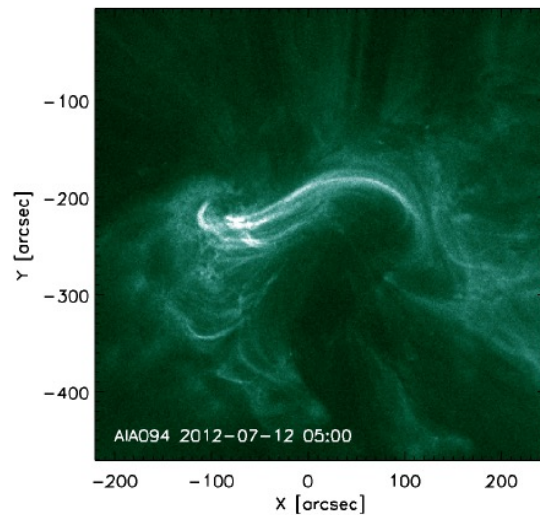


Scolini+ 2019



Input for new generation of CME propagation + flux rope models (e.g., SUSANOO [Shiota & Kataoka, 2016](#); EUHFORIA [Scolini+ 2019, 2020](#)).

Spheromak-type flux ropes easier to handle compared to Gibson-Low.



MHD model input parameters for magnetized CMEs



©C. Scolini

Parameter	Values	Units
CME time	Any date	Date and time (UT)
CME speed	0 ↔ inf	Km/s
CME radius	0 ↔ 21.5	Rs
CME longitude	-180 ↔ +180	degrees (HEEQ)
CME latitude	-60 ↔ +60	degrees (HEEQ)
CME density (uniform)	0 ↔ inf	Kg/m ³
CME temperature (uniform)	0 ↔ inf	K
FR chirality (=helicity sign)	-1 / +1	
FR tilt	0 ↔ 360	degrees
FR toroidal magnetic flux	0 ↔ inf	Wb

White-light images and photospheric magnetograms

EUHFORIA model input parameters + **for magnetized spheromak CMEs**
 (see Scolini+ 2019, 2021 and Verbeke+ 2019)

CME magnetic properties

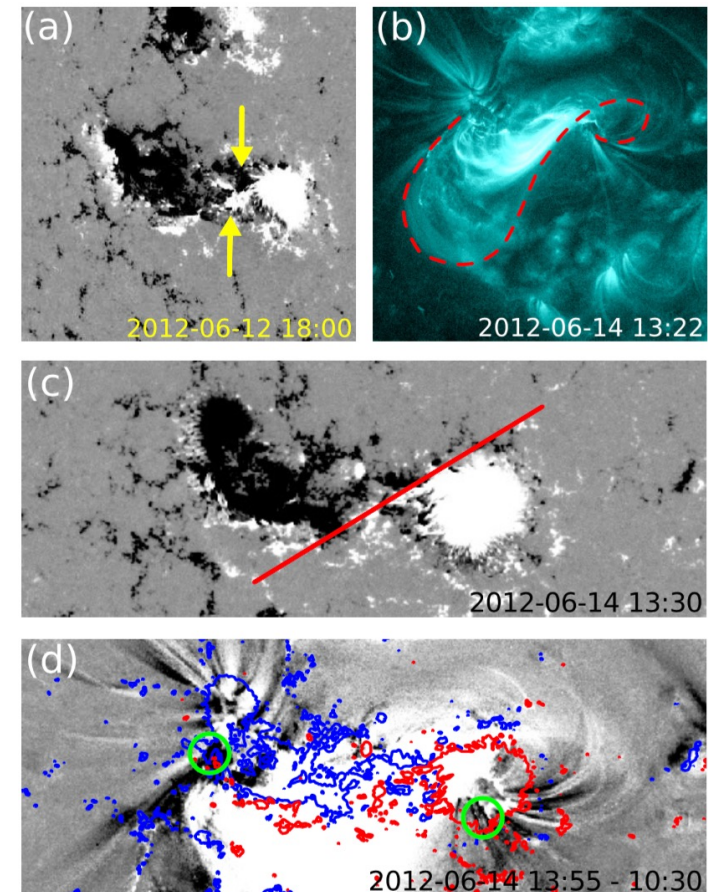


Helicity and initial orientation of the MFR within a CME (e.g., Bothmer & Schwenn, 1998; Wang, 2013; Janvier+ 2014; Temmer+ 2017, Palmerio+ 2018).

Toroidal magnetic flux from flare reconnection (e.g., Möstl+ 2008; Green & Kliem, 2009; 2014; Savani+ 2015; Scolini+2020).

Link remote and in-situ magnetic field (e.g., Mandrini+ 2005; Dasso+ 2005; Patsourakos & Georgoulis, 2016).

Non-eruptive nature of ARs (Thalmann+ 2015; Sun+ 2015).



Palmerio+ 2018

Magnetized ejecta as model input for L1 B_z forecasting – major challenge in predicting geoeffectiveness of CMEs.

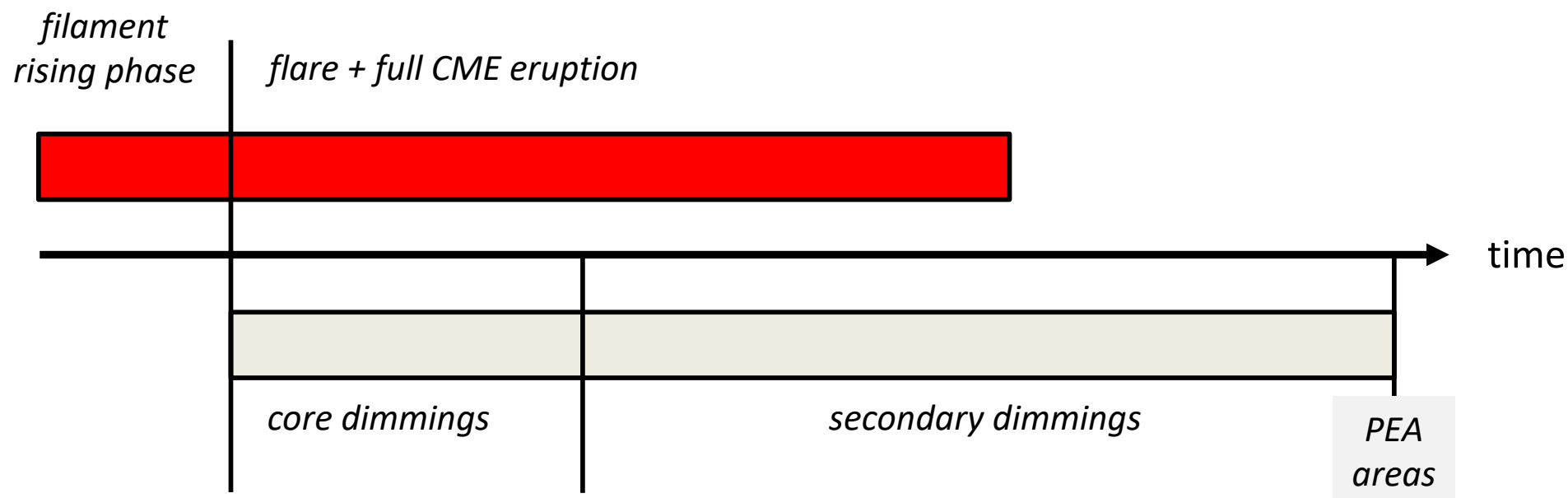
ITY OF GRAZ

Total reconnected flux – input parameter for CME propagation models

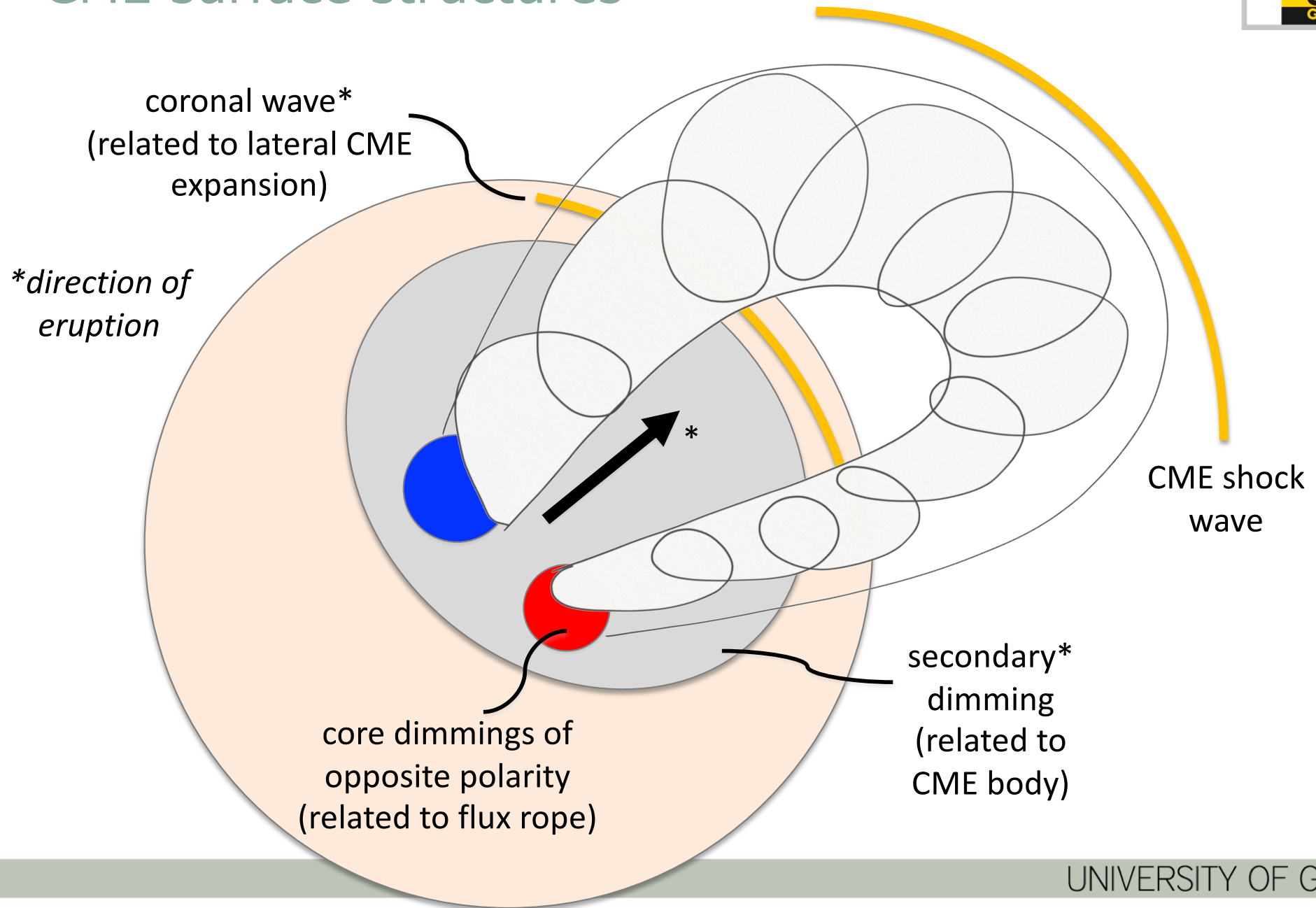
Observational signatures of reconnection areas:

- ✓ filament eruption (timing)
- ✓ flare ribbon areas
- ✓ dimming regions (core and secondary)
- ✓ Post-eruptive arcades (PEA)

- Large uncertainties in deriving the reconnected flux. Results reveal $\pm 50\%$ of the measured value (Gopalswamy+ 2017; Pal+ 2017; Temmer+ 2017; Dissauer+ 2018a; Tschernitz+ 2018).
- Empirical relations provide a fast and easy way to estimate the reconnected flux (see Scolini+ 2020).

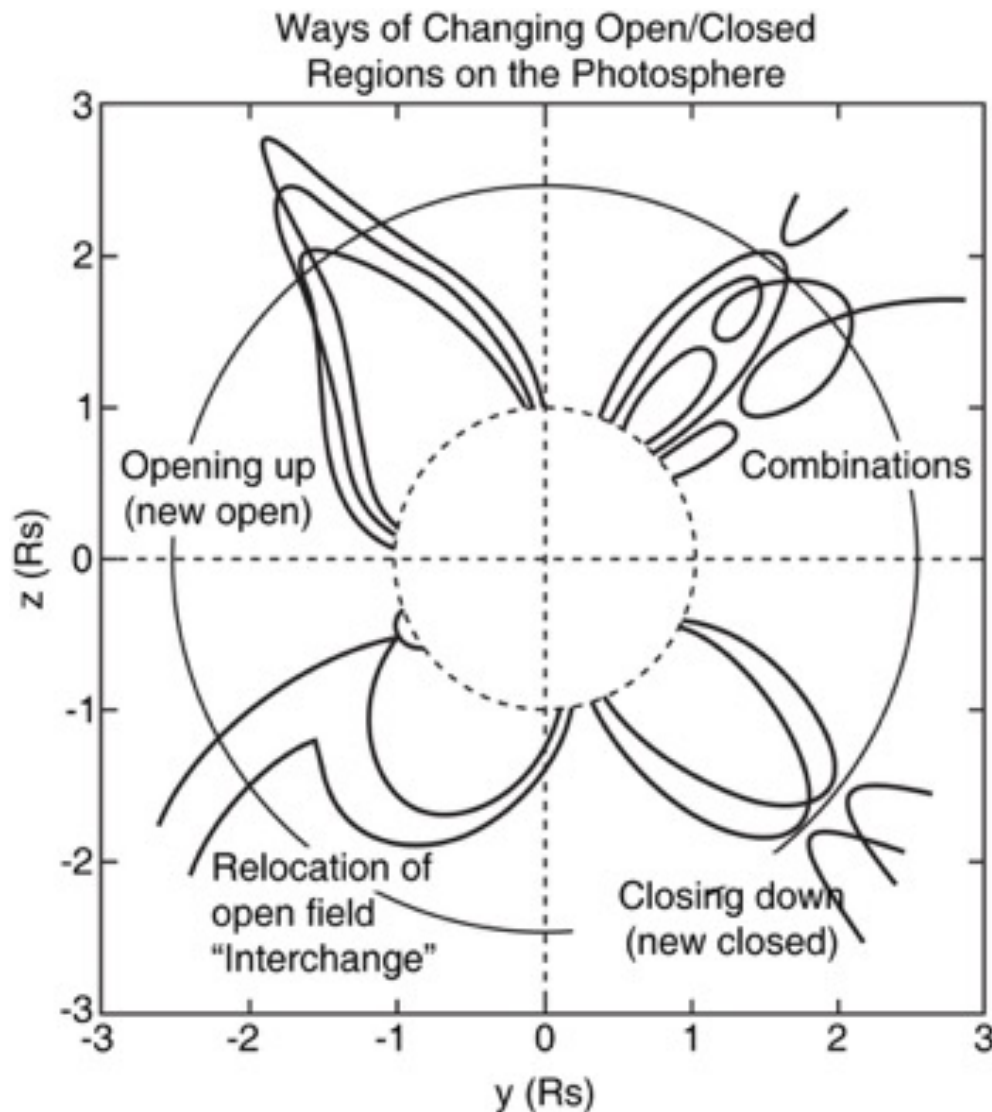


CME surface structures



Solar wind interaction and variations of initial CME parameters

Backbone of Space Weather models: the solar wind



J. Luhmann (Heliophysics Summer School)

The CME provides a way for closed loops to open and open fields to close where required by new boundary conditions, or to reduce magnetic stress (appearing as currents) introduced by field emergence or evolution.

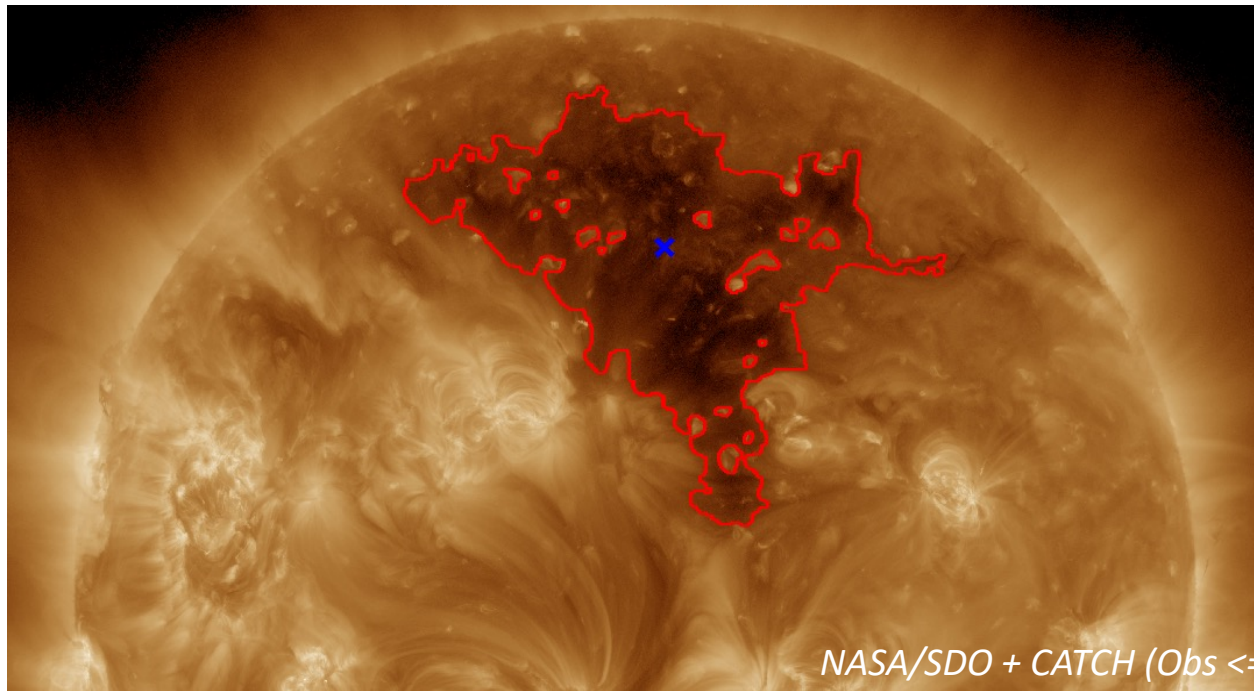
CME propagation in IP space related to the mix of open and closed IMF and flow structures such as stream interaction regions (SIR/CIR).

Review on CME propagation see e.g., [Luhmann+ 2020](#)

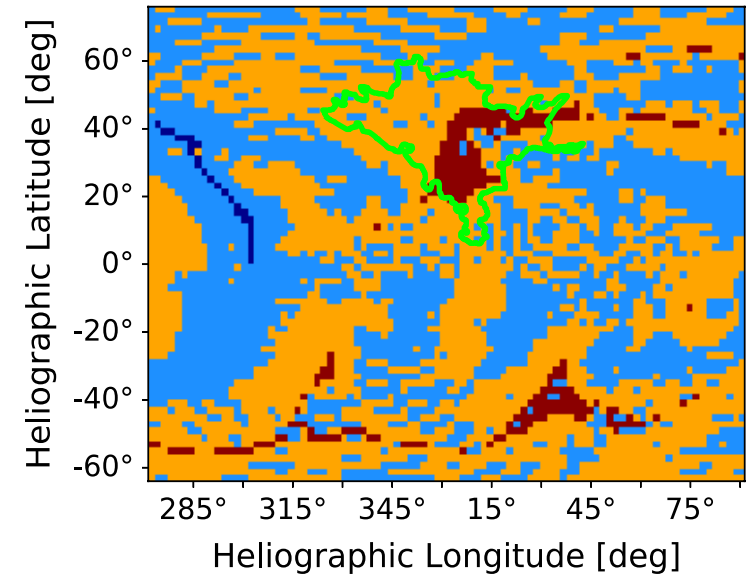
Sources of the solar wind



<http://www.issibern.ch/teams/magfluxsol/>

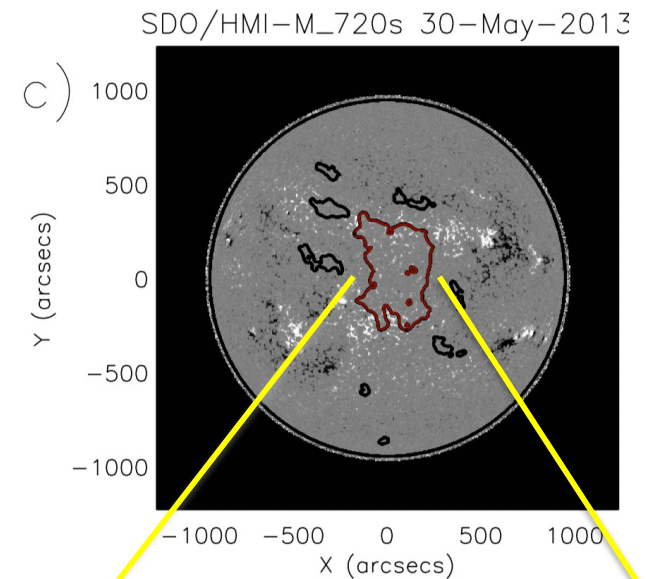
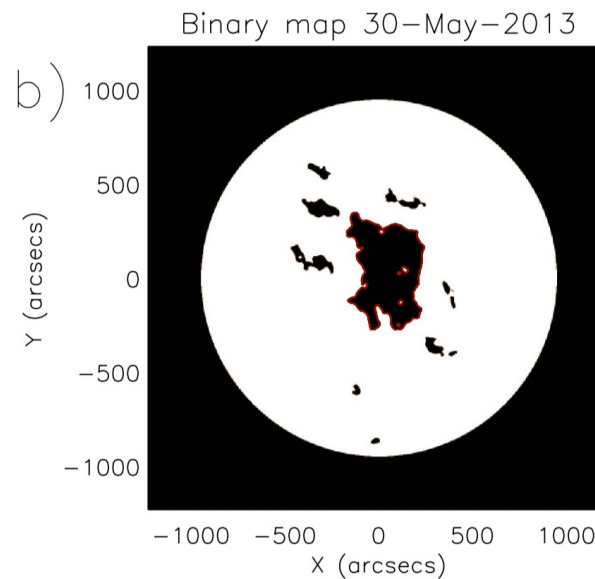
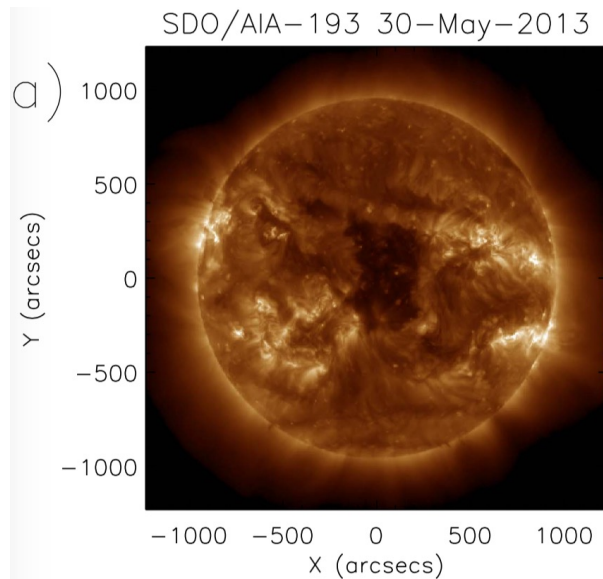


NASA/SDO + CATCH (Obs \Leftrightarrow Model) EUHFORIA



- Mixture of **open and closed magnetic field** - slow and fast wind. Their interaction structures IP space (SIR/CIR - HSSs).
- Studying coronal holes is important
- Comparison to models may be poor: open flux - uncertainties ca. 25% (Linker+ 2021); switchbacks? (PSP: Tenerani+2020, Zank+2020)
- Model validation is key to improve understanding of large-scale structures in IP space and impact at planets

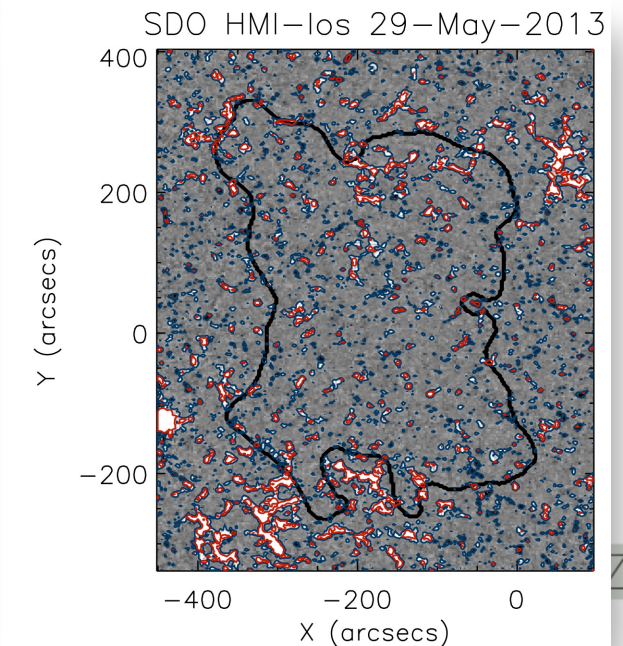
Coronal holes and their fine structure



Open field predominantly concentrated in unipolar magnetic flux tubes inside CHs:

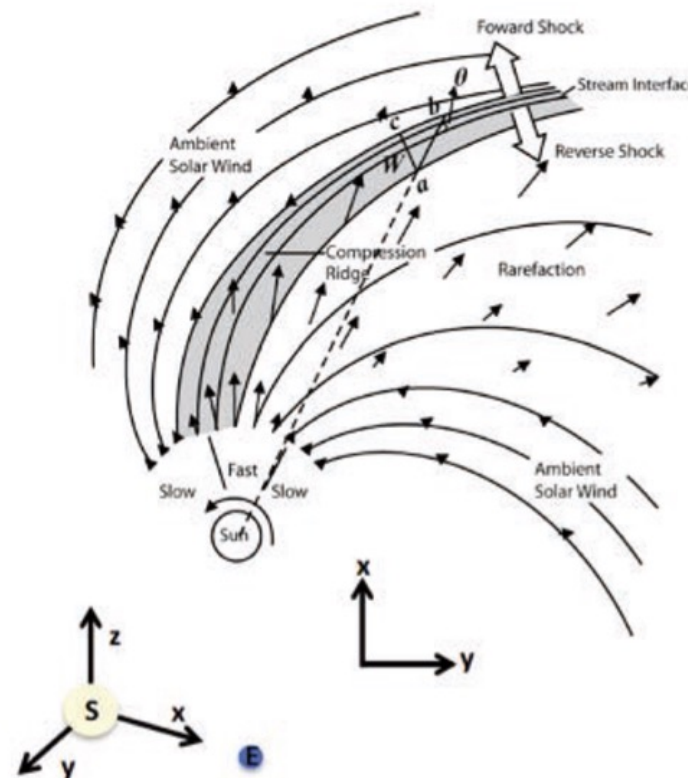
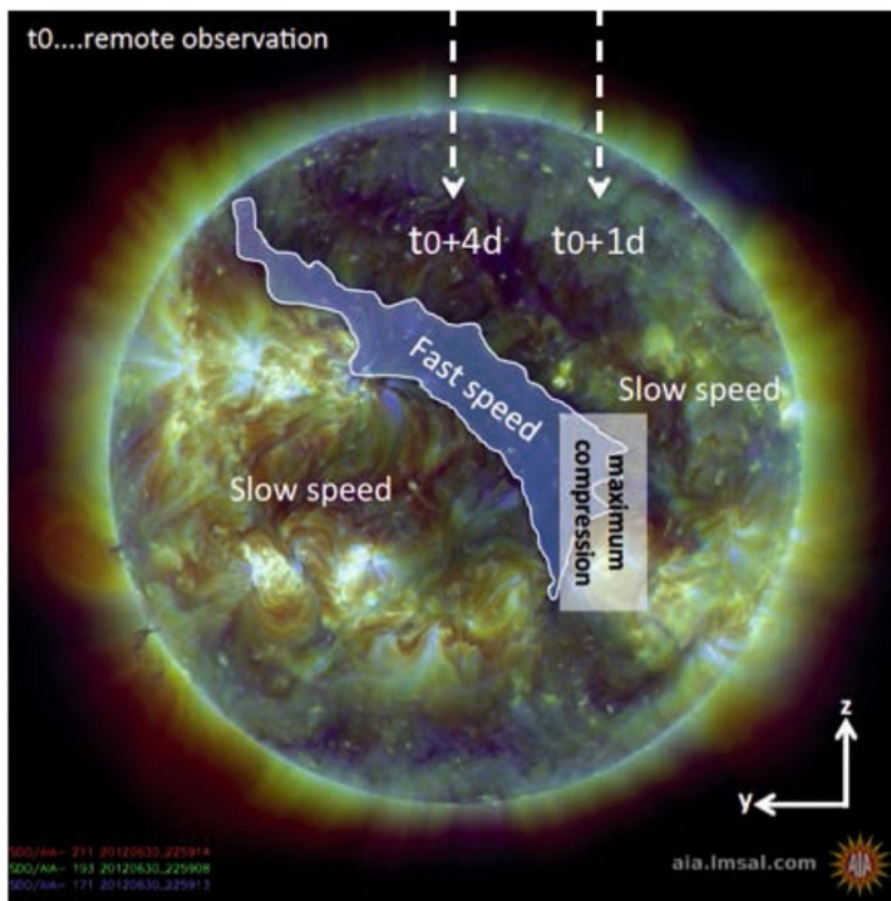
- 38% (81%) of the unbalanced magnetic flux of CHs arises from only 1% (10%) of the CH area with
- magnetic flux tubes of field strengths >50 G (10 G).
See [Hofmeister+ 2017, 2019](#); [Heinemann+ 2018](#);

Evolution of CH boundaries and coronal bright points ([Madjarska & Wiegelmann 2009](#); [Madjarska 2019](#)).



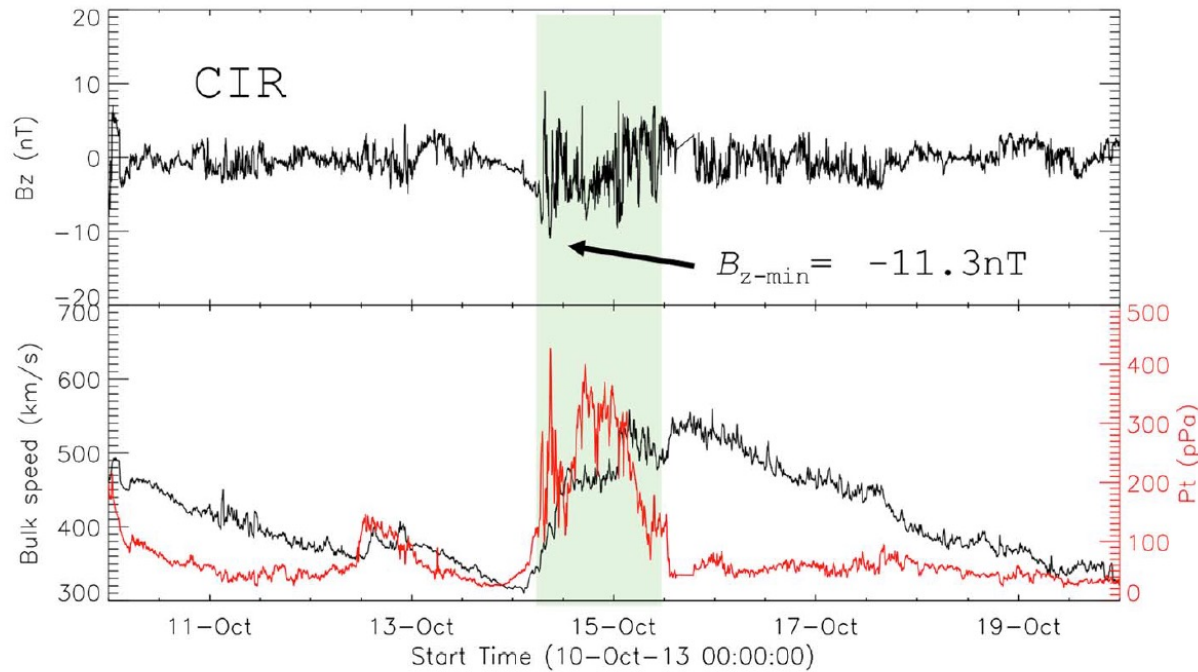
The fast solar wind and open field

Temmer, 2021 (Liv.Rev.)

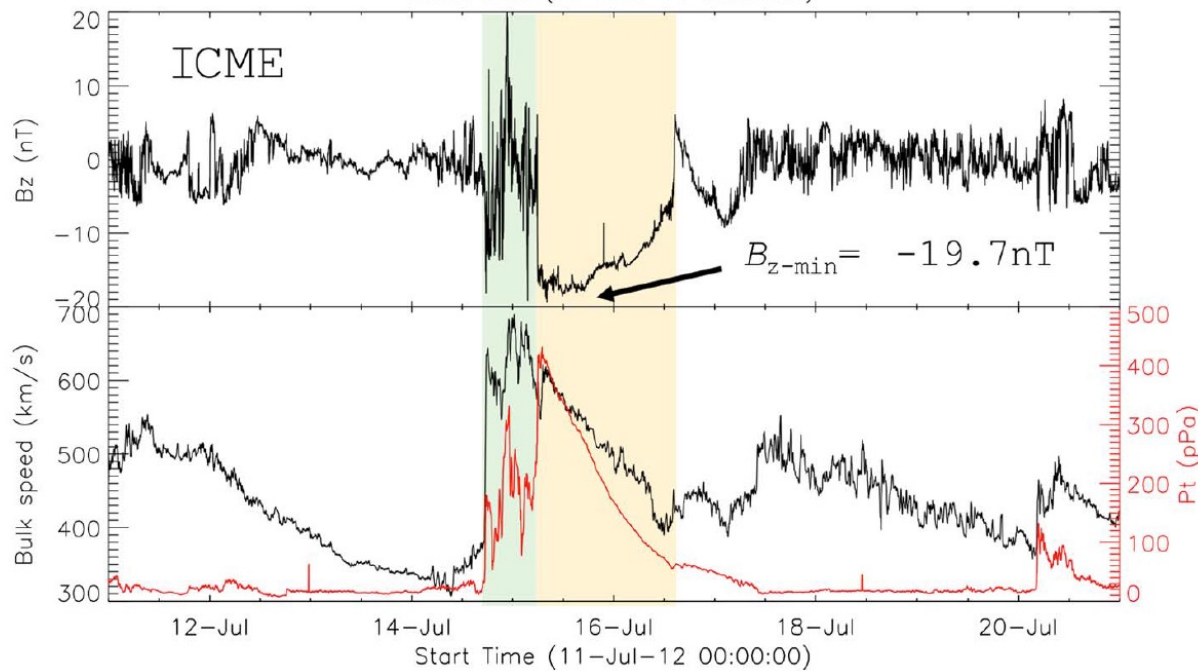


Left: SDO/AIA composite image showing the reduced density region of a coronal hole (shaded area). At the time t_0 , the coronal hole reaches a central position. From in-situ data at 1 AU about 1 day later the maximum in the density/magnetic field is measured (SIR; stream interaction region) and about 4 days later the maximum in the speed/temperature (HSS; high speed stream).

Right: Fundamental processes; adapted from Pizzo (1978).



Compression regions from SIR/CIRs and the shock-sheath component of a CME (green shaded areas) cause similar (weak) effects in the thermospheric density enhancements.



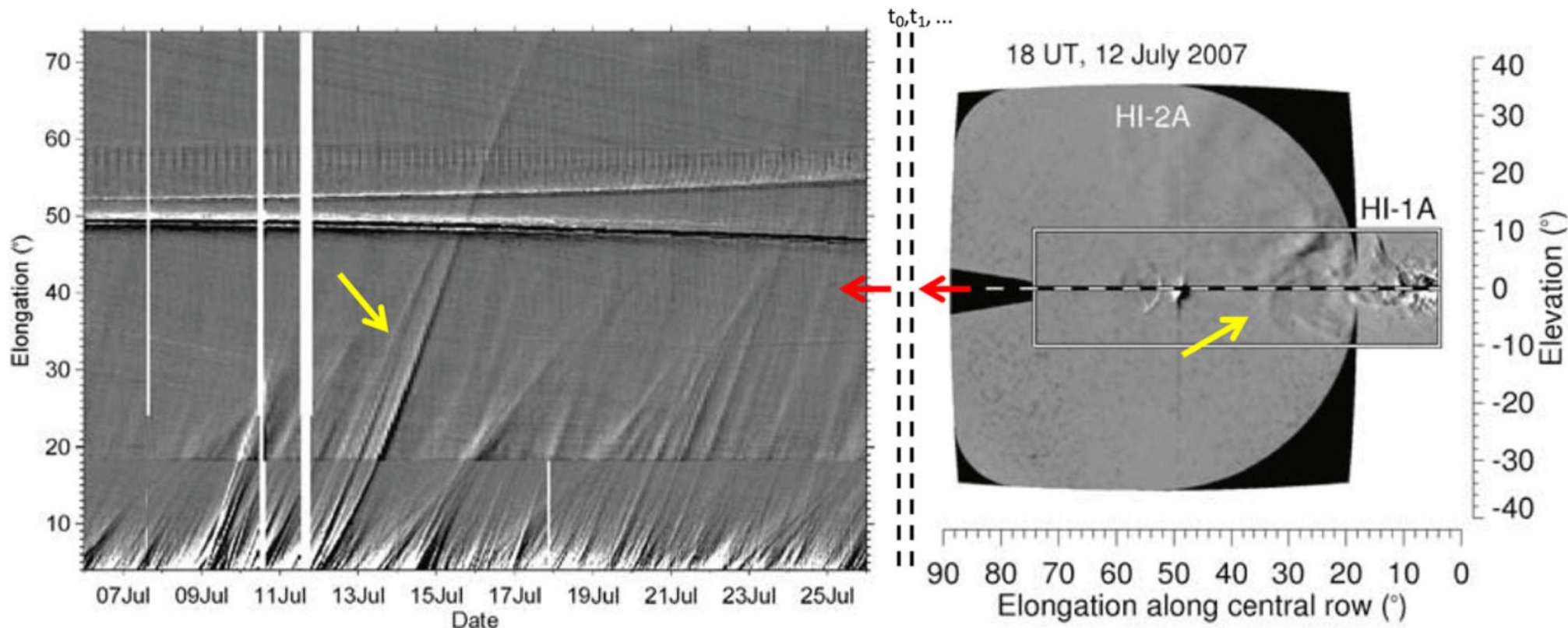
The strong magnetic field in the flux rope causes major geomagnetic effects.

See more on CME sheath formation [Temmer+ 2021 \(JGR\)](#)

Heliospheric Image Data aboard STEREO

Time-elongation plots (so-called Jmap) show the CME propagation in IP space. The CME front is marked by a yellow arrow in the direct image (right panel) as well as in the Jmap. View off the CME propagation line is necessary.

Future mission ESA/Vigil located at L5.

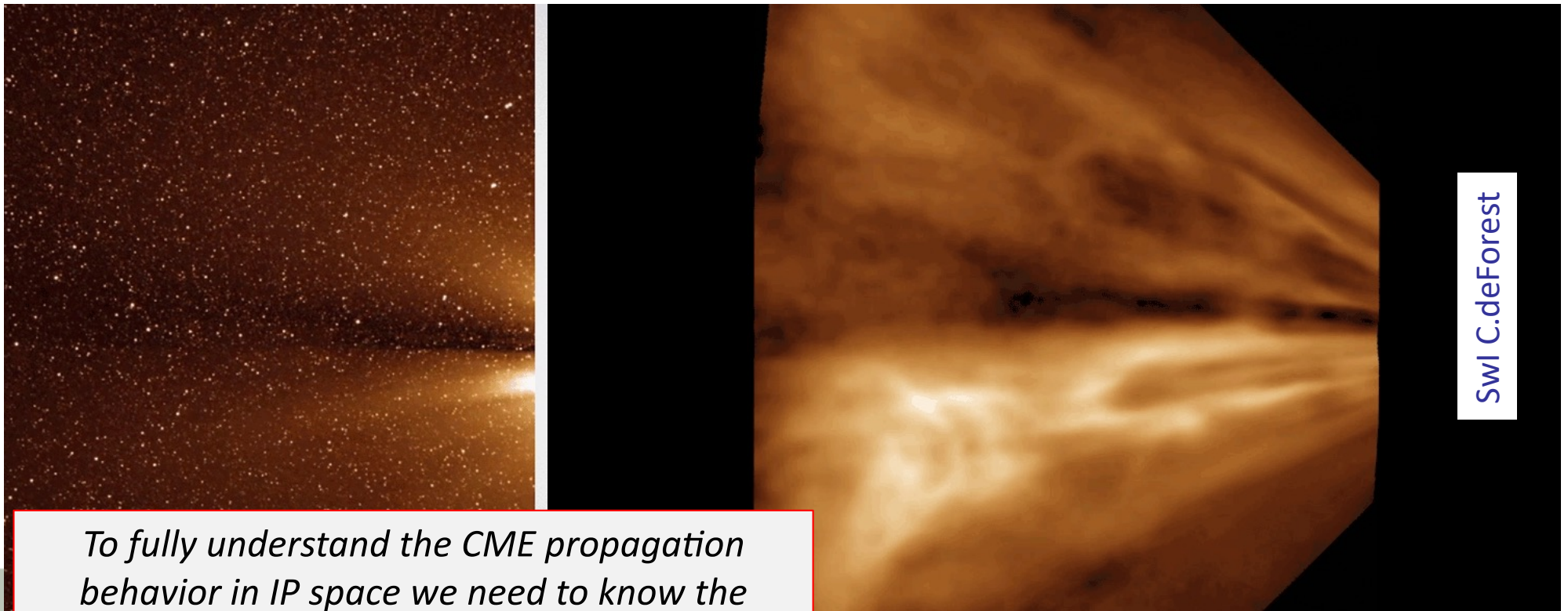


Temmer, 2021 (Living Reviews) adapted from Davies+ (2009)

CMEs and background solar wind interaction: change of direction/orientation



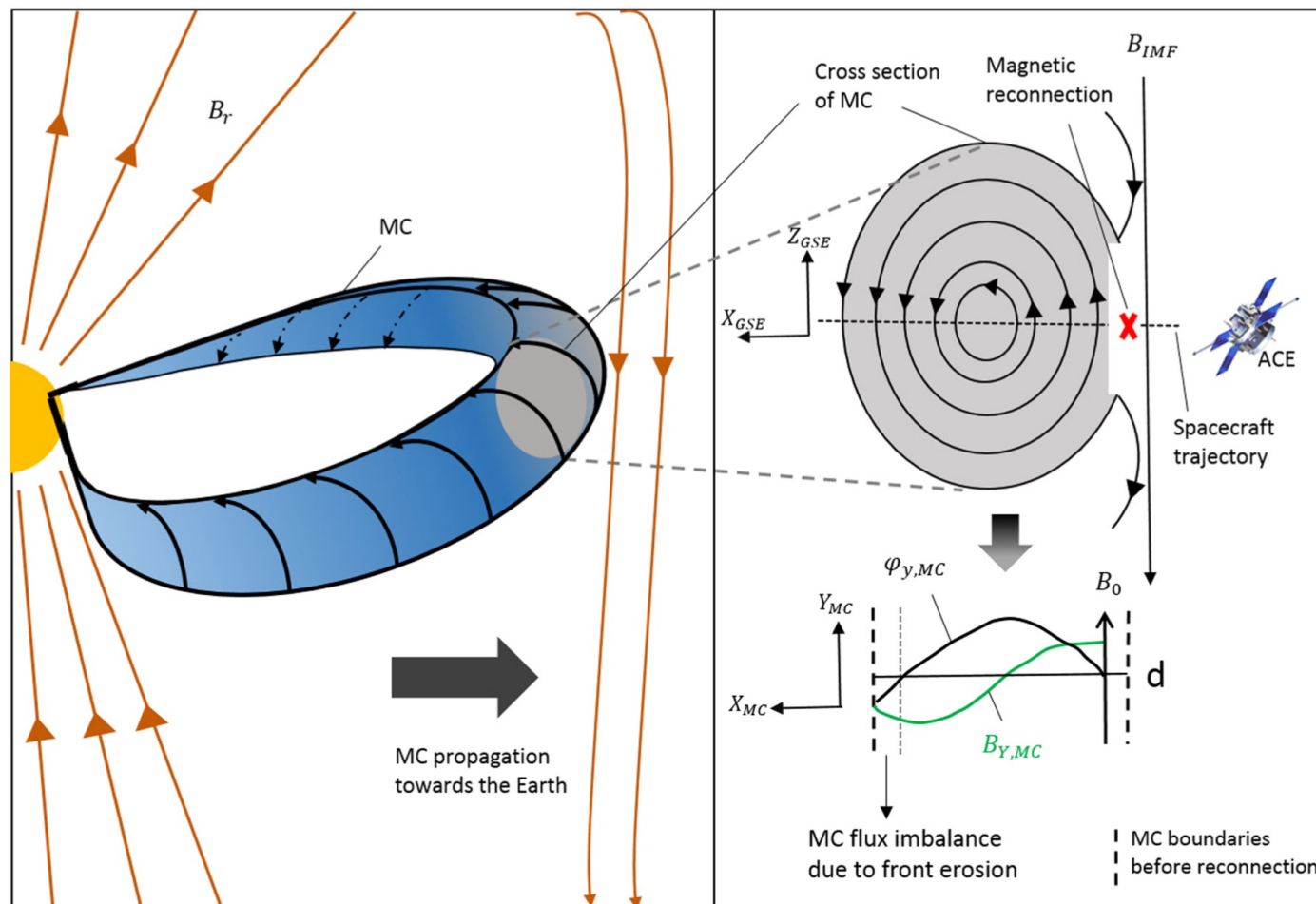
- CME rotation and adjustment to ambient magnetic field (pressure gradients) as well as flow speed (e.g., Yurchyshyn+ 2001; 2009; Vourlidas+ 2011; Isavnin+ 2014)
- Latitudinal/longitudinal deflection/channeling in corona (e.g. Bosman+ 2012; Panasenco+ 2013; Wang+ 2014; Möstl+ 2015; Harrison+ 2018)
- Location of coronal holes are important (Gopalswamy+ 2009)



SwI C.deForest

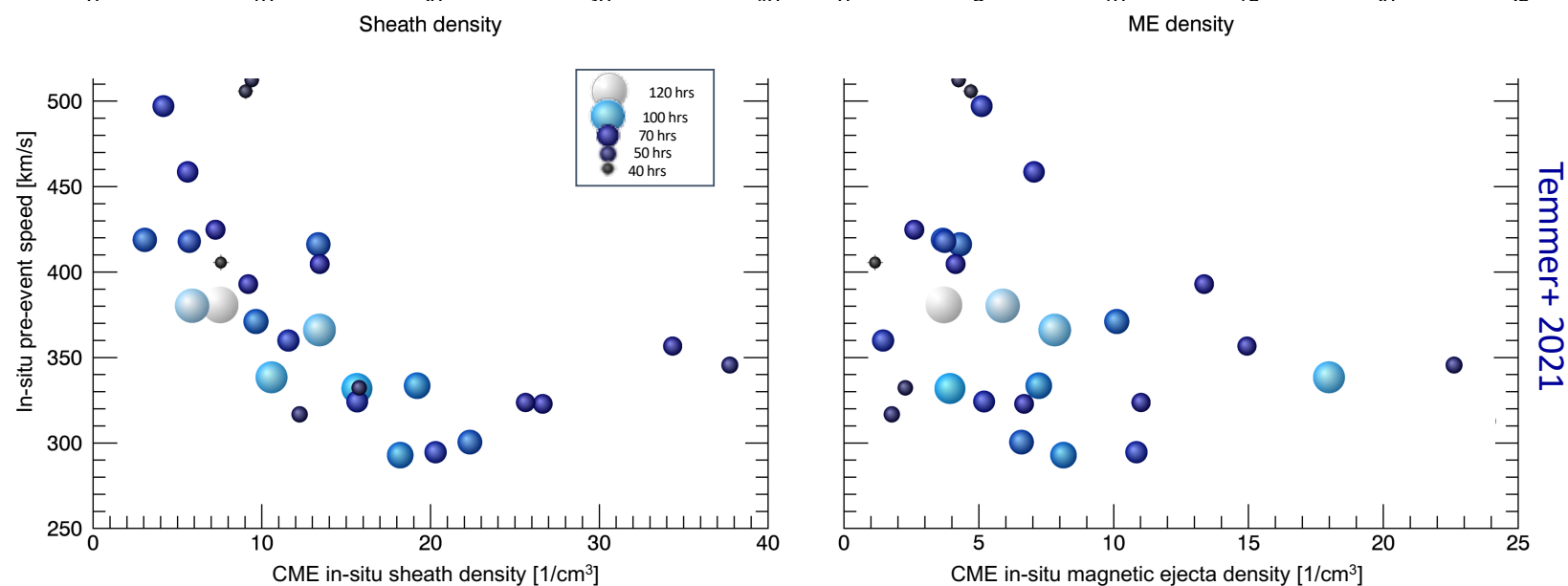
*To fully understand the CME propagation behavior in IP space we need to know the **spatial distribution of SW parameters.***

IMF and CMEs magnetic structure: flux variation



Idealized schematics of the ambient IMF draping around the propagating magnetic structure (magnetic cloud, MC). Variations in the Mc's accumulated azimuthal flux due to possible reconnection with the draped ambient IMF. From [Pal+ 2020](#)

CME sheath region: mass variation



- CMEs increase in mass up to $20R_s$ coming from surface outflows (Bein+2013, Howard & Vourlidas2018)
- In IP space, sheath formation due to SW pile-up (e.g., deForest+2013; Kilpua+ 2017).
- Relation with the ambient solar wind speed (Temmer+2021); **sheath build up** might start around $13R_s$ (Helios1/2 data, Temmer&Bothmer2022 under rev. for A&A, PSP will show more...stay tuned!).
- A change in mass/density relates to the effectiveness of the drag force. More massive CMEs show low deceleration (Vrsnak+2010).

CME-CME/CME-SIR interaction events

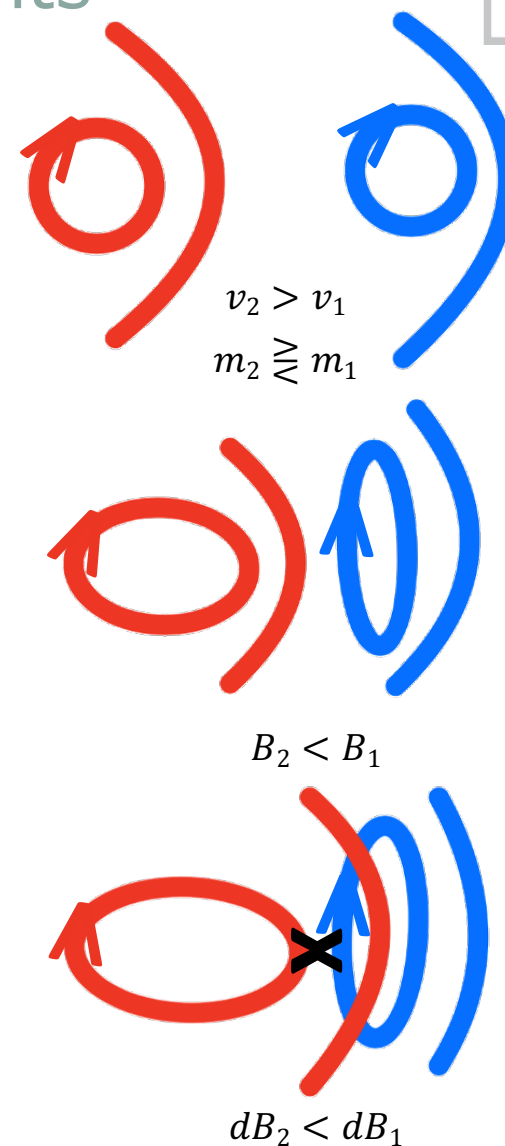
Merged CMEs form complex ejecta of single fronts (e.g., Gopalswamy+ 2001; Burlaga+ 2002, 2003; Harrison+ 2012).

Change in kinematics, deflection,... (e.g., Farrugia & Berdichevsky, 2004; Temmer+ 2012, Lugaz+ 2015, Mishra+2018).

Increased B fluctuations and extended periods of neg. B_z (e.g. Wang+ 2003; Farrugia+ 2006; Scolini+ 2020).

⇒ **Most intense geomagnetic storms** (Burlaga+ 1987; Farrugia+ 2006a,b; Xie+ 2006; Dumbović+ 2015)

⇒ CME-CME interaction review by Lugaz, Temmer, Wang, Farrugia, in *Solar Physics* (2017)



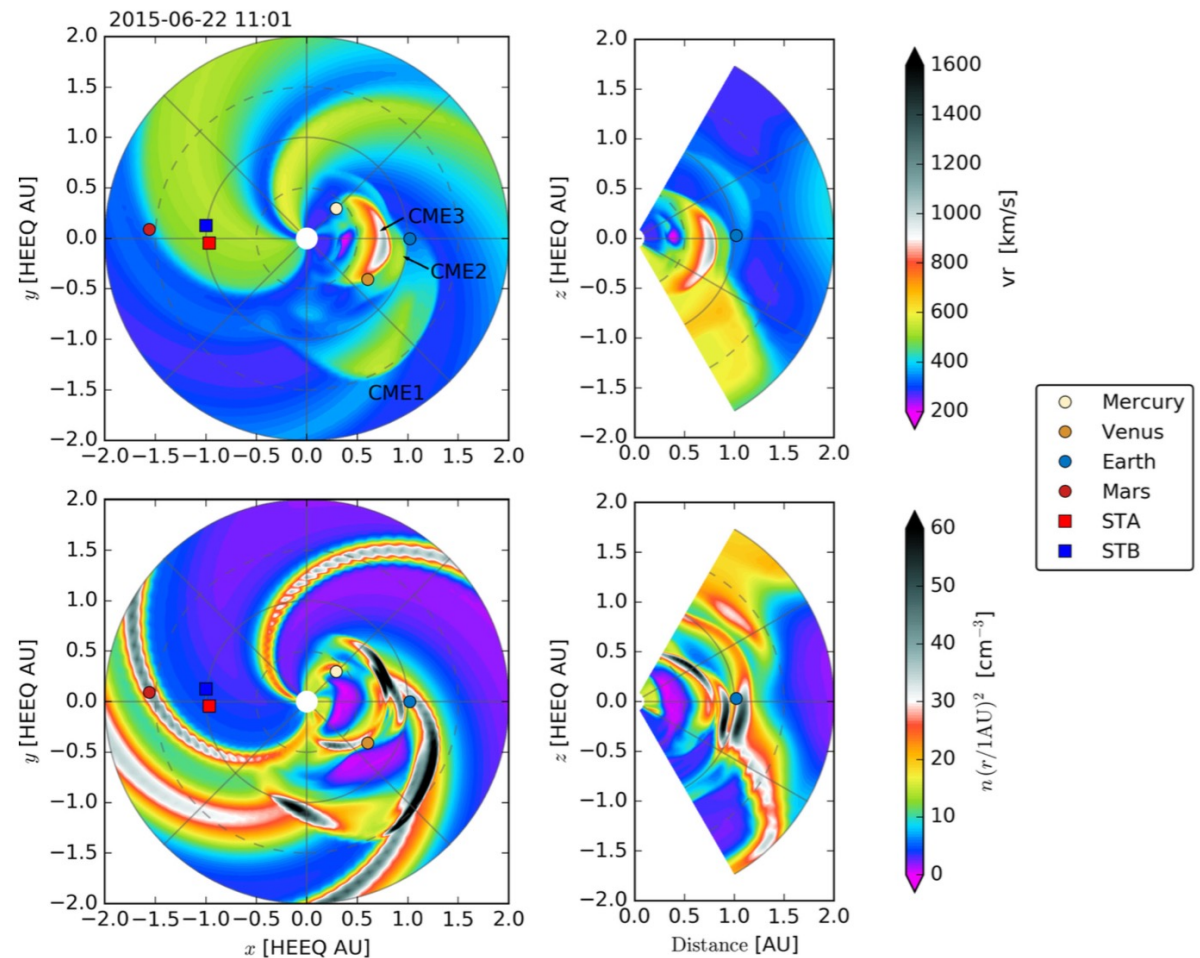
Preconditioning – rule or exception?

EUHFORIA (Pomoell & Poedts 2018); ENLIL (Odstrcil+ 2002)

CME occurrence rate: 2-3/w (solar min) to 4-5/d (solar max) (e.g., St. Cyr+ 2000, Gopalswamy+ 2006).

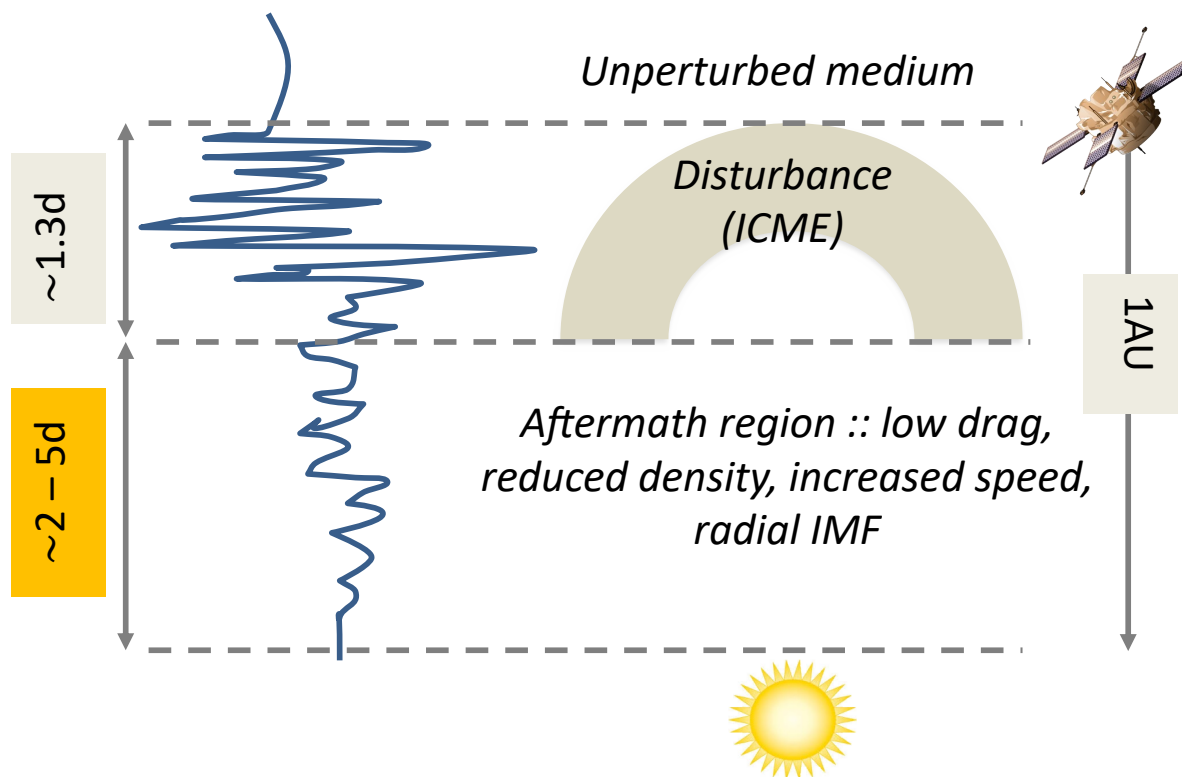
CME 1AU tt : 1 to 4 days (close to Sun: mean v : 500 km/s; max. v up to 3000 km/s).

2 – 20 CMEs within Sun-Earth sector, depending on solar cycle phase (Lugaz+ 2017).



During times of increased solar activity, „CME-chains“ are assumed to happen frequently. Effects on model performance (Gressl+ 2014).

Preconditioning of IP space



- Drag might be lowered by factor of 10 due to preceding CME (Temmer & Nitta, 2015) and B is more radial (Liu+ 2014).
- September 4-6, 2017 events high impact due to CME-CME interaction close to Earth (Werner+ 2019; Scolini+ 2020)

IP space needs ca. **2-5 days** to „recover“ from strong disturbances (Temmer+ 2017; Janvier+ 2019)

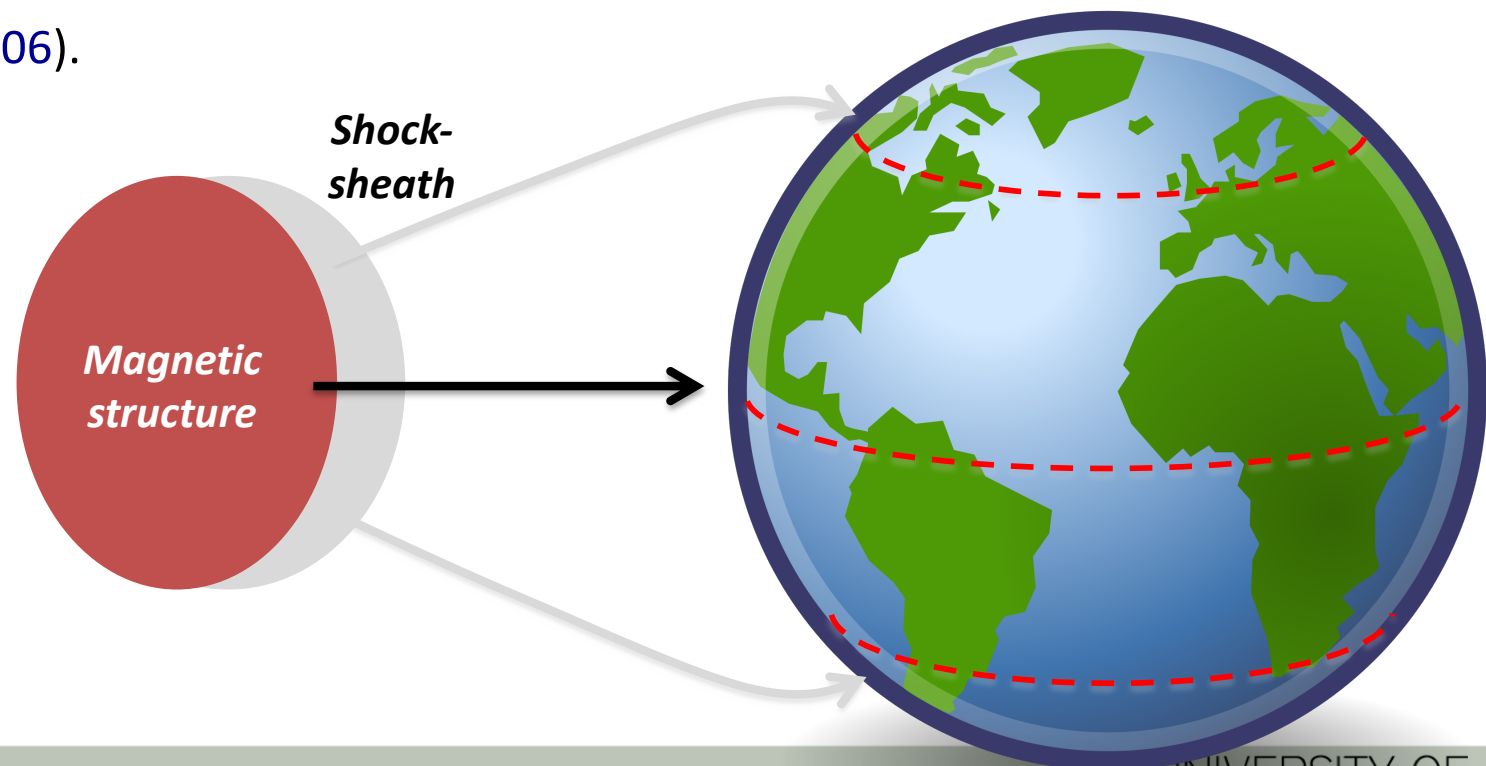
To improve models/predictions and to better understand, take into account ALL disturbances leaving Sun at least 2 days and up to 5 days before the actual event of interest.

Impact at Earth – interdisciplinary research!

Cascade of reactions in the magnetosphere (substorms), ionosphere (dB_z/dt), thermosphere (satellite drag), GICs, ...

Differences in magnetospheric response between ICMEs and shock-sheath regions (e.g., Huttunen+ 2005, 2008; Krauss+ 2015; Kilpua+2017).

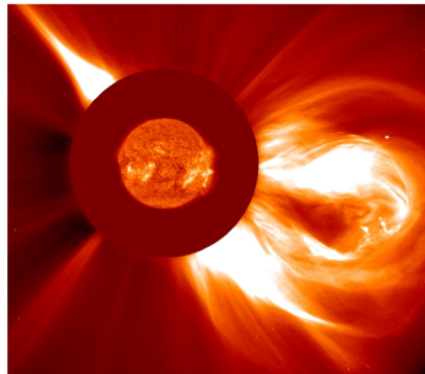
Differences between CME and CIR-driven storms (Borovsky+2006).



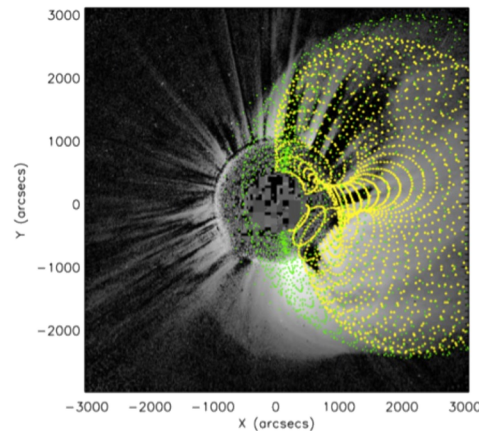
Forbush decrease - reducing the radiation from CR



REMOTE OBSERVATION

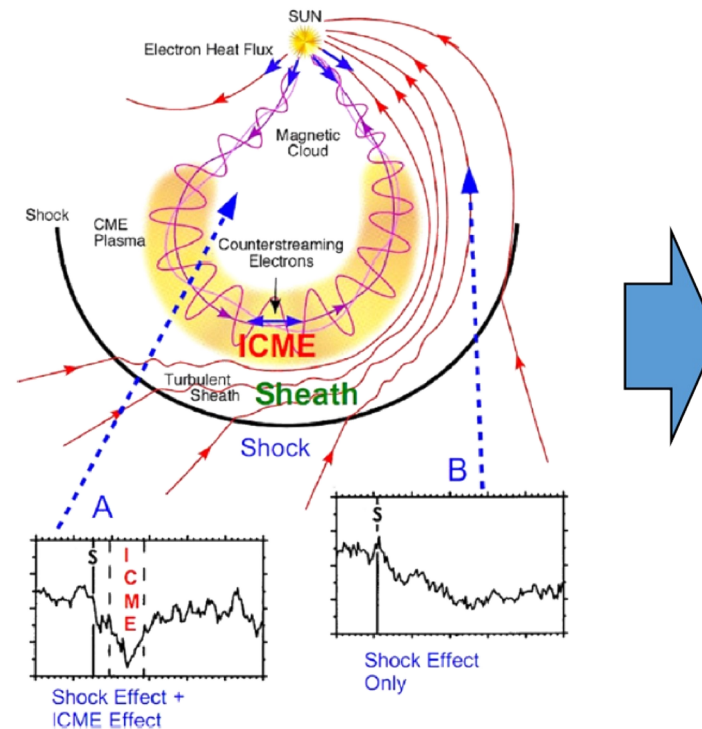


SOHO/LASCO C2 image



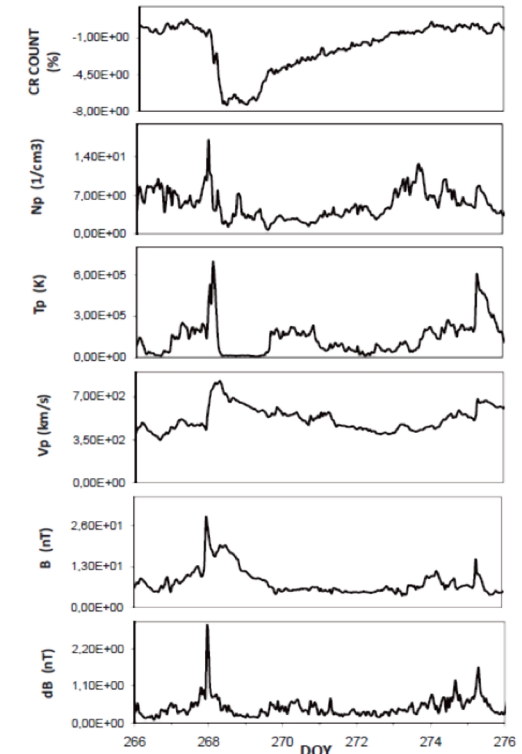
Temmer & Nitta (2015)

VISUALISATION



Richardson & Cane (2011)

IN SITU MEASUREMENTS

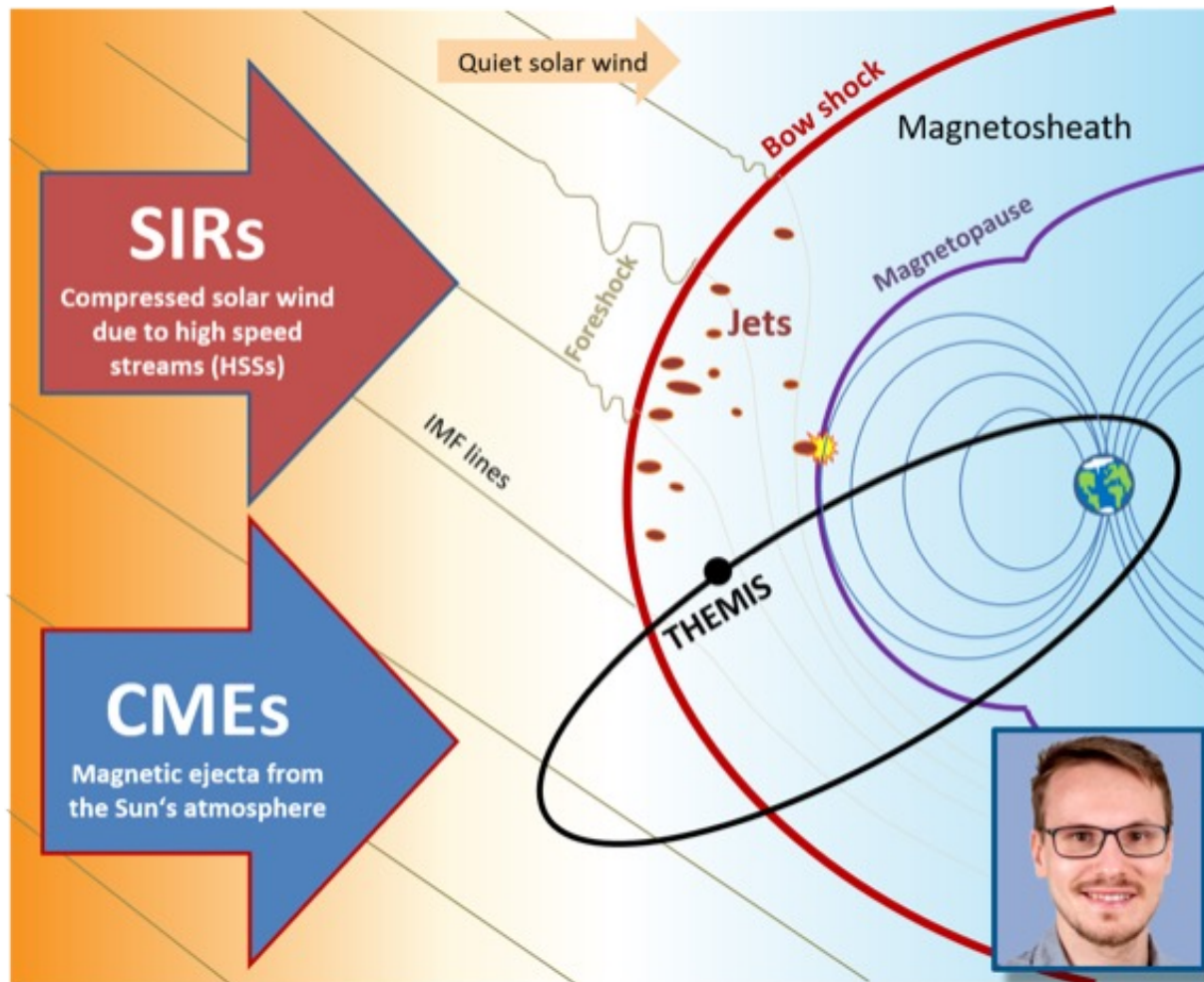


Dumbovic et al (2012)

2-step Forbush decrease caused by ICMEs and reduces cosmic ray (CR) radiation:

- 1) shock/sheath region highly turbulent strong B -> fast decrease, prolonged recovery
- 2) CME ejecta (magnetic cloud, flux rope) smooth & strong B fluctuations very low -> Symmetric-like decrease, timespan limited to the ejecta
- Also observable at Mars (see e.g., [Papaioannou+ 2019](#))

Magnetosheath jets – Space Weather relevant!



Florian Koller, PhD student Graz

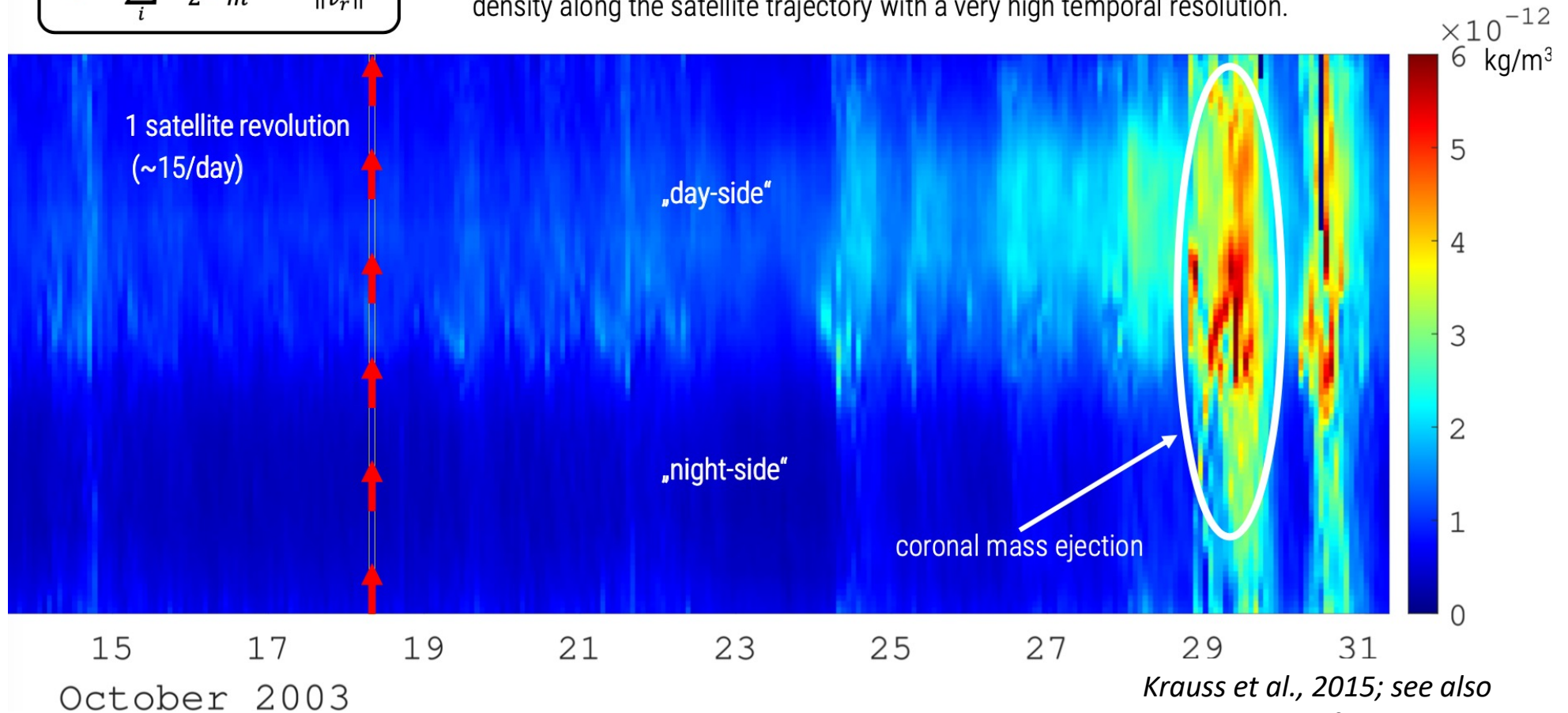
- Magnetosheath jets constitute a significant coupling effect between SW and the Earth's magnetosphere (e.g., [Hietala+2009](#); [Plaschke+2018](#)).
- Recent studies showed a clear variation with incoming large-scale SW structures SIRs and CMEs ([Koller+ 2022](#)).
- Effect on planetary atmosphere not fully understood

Neutral density enhancement in the thermosphere



$$\vec{a}_a = \sum_i -\frac{1}{2} \rho \frac{A_i}{m} C_F v_r^2 \frac{\vec{v}_r}{\|\vec{v}_r\|}$$

Based on accelerometer measurements we can monitor the neutral mass density along the satellite trajectory with a very high temporal resolution.

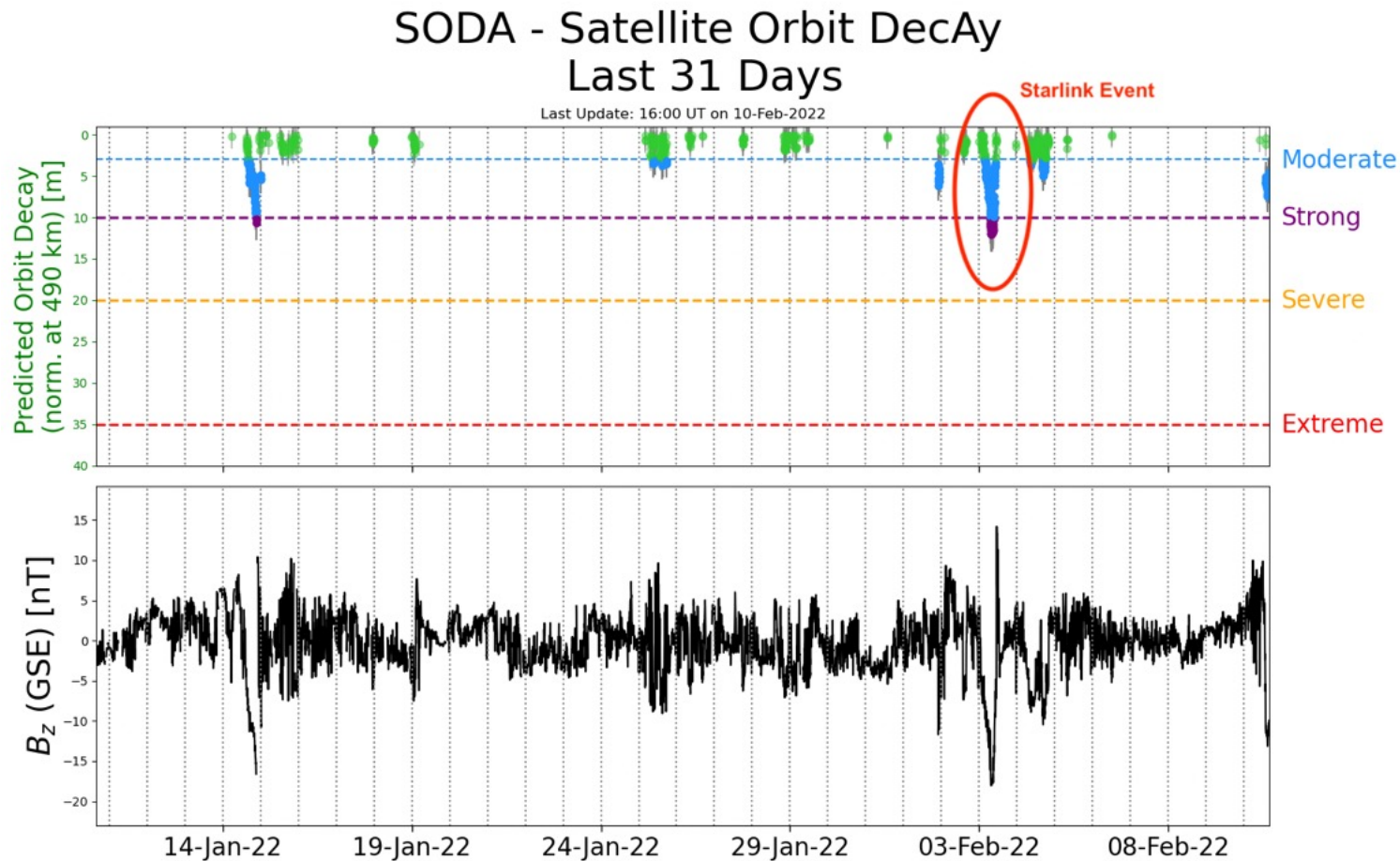


*Krauss et al., 2015; see also
EGU Campfire 2022*

Thermosphere neutral density response to CMEs and CIRs (e.g., Knipp+ 2004; Bruinsma+2006; Krauss+ 2015, 2018, 2020).

Energy input via Joule heating – relation to MS jets possible

Loss of Starlink satellites in February 2022



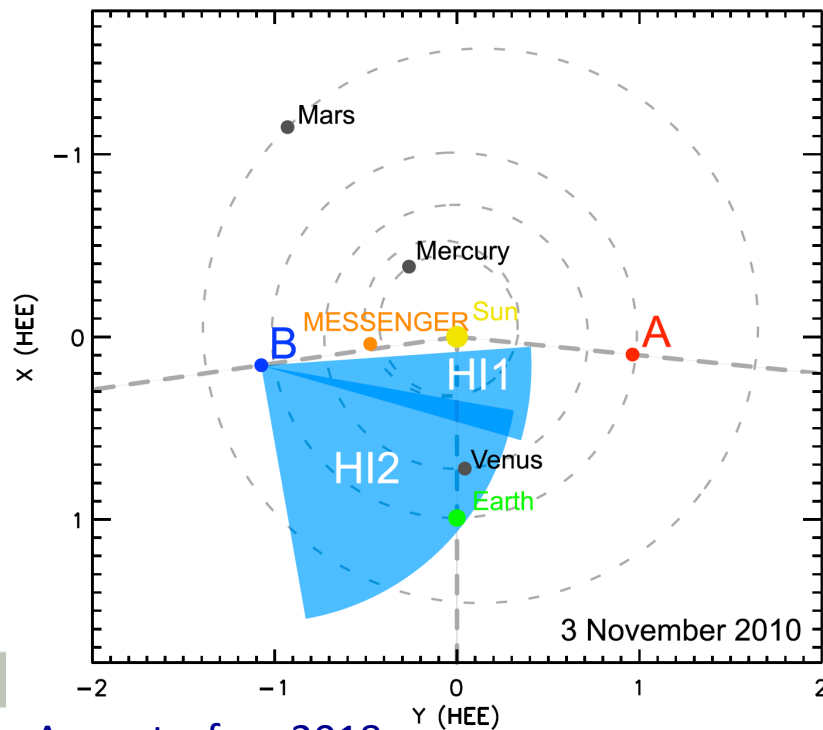
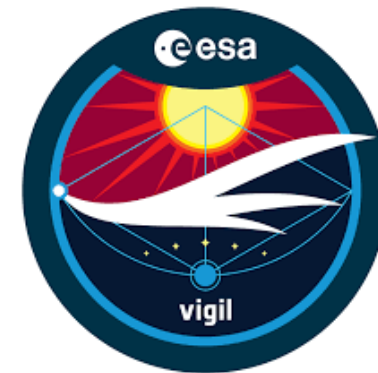
SODA – ESA service (UNI Graz and TU Graz; FFG project SWEETS)

see also <https://swe.uni-graz.at/index.php/services/esa-space-safety-services>

Enhanced knowledge and data to
improve Space Weather models

Advantage of multiple views - L5 mission

- Constrain projection effects, increase surface coverage for magnetic field data
- L4/L5, off-ecliptic provide **continuous monitoring** of interplanetary space (Vigil)
- However, hard to distinguish structures using image data
- Enable connecting large-scale structures in image data to small scale measured in-situ



Event studies using STEREO-B close to L5 position (2009-2010) revealed advantages in the analysis and understanding.

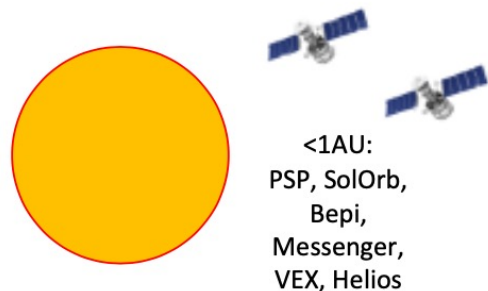
Tracking of evolving structures over radial distance with VEX, MESSENGER, MAVEN, PSP, Solar Orbiter...

Summary and conclusions



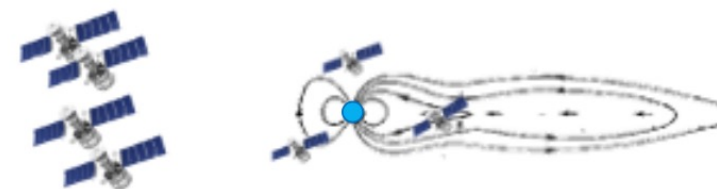
- CME properties are set in the low corona -> source region characteristics, magnetic reconnection process linking flares, filaments, dimmings, CMEs
- Ambient magnetic field configuration controls CME onset (confined versus eruptive) and propagation behavior (magnetic pressure gradient)
- Propagation behavior of CMEs in IP space strongly affected by the characteristics of the ambient solar wind flow – structures (SIRs/CIRs)
- CME-CME interaction and preconditioning: extreme changes in CME dynamics; model efforts for better understanding the physics and forecasting purposes (ENLIL, EUHFORIA, SUSANOO, EIEvoHI, ...)
- Challenge: input parameters for models (uncertainty assessment); open magnetic flux, magnetic properties of CMEs; *international teams!*

iSWAT – international Space Weather action teams where interdisciplinary research meets



*Solar wind, SIR, HSS
CME, ICME
Mutual interaction
(SEP propagation)*

L1:
ACE, Wind,
DSCOVR, STA



Sun (S)

- Dynamic (recurrent) interplay between open and closed magnetic field (SIR/CIR, HSS)
- Short-term variations (flare, CME, SEP)
- Long-term variations (solar cycle)

Heliosphere (H)

- Structure and evolution of IP space (variations on different spatial and temporal scales)
- SIRs/CIRs formation and propagation (including arrival characteristics at targets)
- CME propagation behavior (drag force, arrival characteristics at targets)
- Interaction phenomena (HSSs-CMEs, CIRs/SIRs-CMEs, CME-CME)
- Data and models
- Metrics and validation procedures

Geospace (G)

- Energy input
- Magnetosphere coupling
- Ionosphere, Thermosphere
- Ground effects (GIC)

Input to H-models
CME: magnetic field, speed, size, location; background solar wind, SIR/CIR location, ...

Output from H-models
impact and arrival characteristics of CMEs/transient events and HSSs/SIRs/CIRs

Give it a try!

<https://swe.ssa.esa.int/heliospheric-weather>



Drag-Based (Ensemble) Model - DBEMv3 with GCS of probabilistic model for heliospheric propagation of C

Input
Documentation

CME date (at R_0): May 27 2021

CME time in UTC (at R_0): 07 h 31 min

Drag parameter, γ (depending on CME speed): 0.2 (normal CME) $\times 10^{-7} \text{ km}^{-1}$

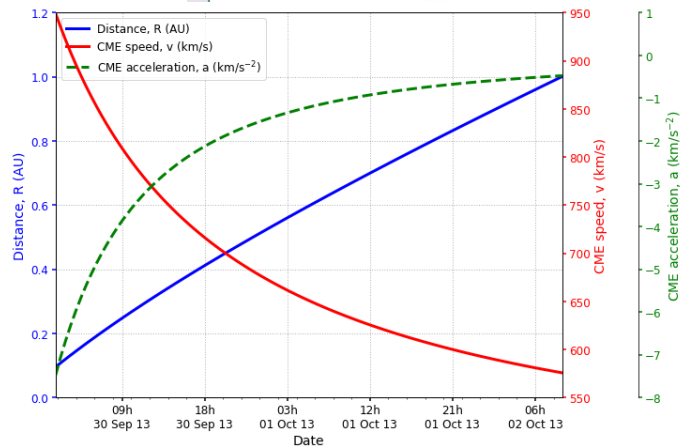
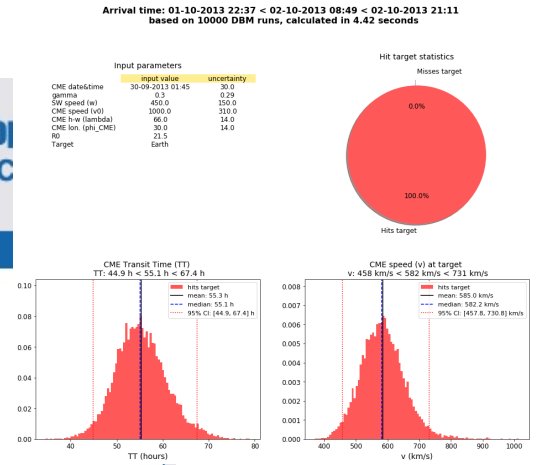
Solar wind speed, w : 450 km/s (current: 272 km/s)

CME starting radial distance, R_0 : 20 r_{Sun}

Starting speed of CME, v_0 (at R_0): 1000 km/s

CME's angular half-width, λ : 30 deg GCS input

Longitude of CME source region, ϕ_{CME} : 0 deg



Input parameters
 CME date & time: 30 Sep 2013 01:45 h
 Drag parameter, γ : $0.3 \times 10^{-7} \text{ km}^{-1}$ | Solar wind speed, w : 450 km/s | Radial distance, R_0 : 21.5 r_{Sun}
 CME initial speed, v_0 : 1000 km/s | CME half-width, λ : 66.0 deg | CME longitude, ϕ_{CME} : 30.0 deg | Target: Earth

figure generated with DBEMv3

Select target: Earth

DBM and set DBEM uncertainties Reset

